Microbially Derived Energy

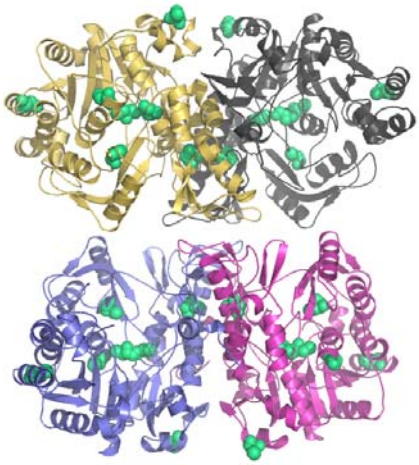

FTHFS 1

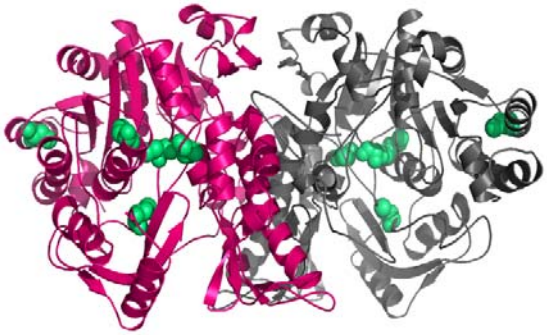

FTHFS 2

Characterization, crystallization and two three dimensional structures of the N^{10}- formyltetrahydrofolate synthetase (FTHFS) from the syntrophic acetate oxidizing bacterium *Tepidanaerobacter acetatoxydans Re1*.

Roland Bergdahl

Department of Molecular Biology, Swedish University of Agricultural Sciences, Uppsala, Sweden
Independent Project in Biology E, 30 HEC, EX0565
Master program in Biotechnology

Autumn 2012, SLU

Characterization, crystallization and two three dimensional structures of the N^{10}-formyltetrahydrofolate synthetase (FTHFS) from the syntrophic acetate oxidizing bacterium *Tepidanaerobacter acetatoxydans Re1.*

Roland Bergdahl

Supervisor:	Nils Egil Mikkelsen, Swedish University of Agricultural Sciences, Department of Molecular Biology
Examiner:	Mats Sandgren, Swedish University of Agricultural Sciences, Department of Molecular Biology

Credits: 30 hec
Level: Second cycle, A2E
Course title: Independent project in Biology – Master's thesis
Course code: EX0565
Program/education: Master program in Biotechnology
Place of publication: Uppsala
Year of publication: 2012
Picture Cover: Roland Bergdahl
Online publication: http://stud.epsilon.slu.se

Key Words: *Biogas, Syntrophic acetate oxidizing bacteria, Tepidanaerobacter acetatoxydans Re1, FTHFS, N^{10}- formyltetrahydrofolate synthetase, Crystallography, Structure determination*

Sveriges lantbruksuniversitet
Swedish University of Agricultural Sciences

Faculty of Natural Resources and Agricultural Sciences
Department of Molecular Biology

Table of contents

Abstract

The crystal structure of N^{10}- formyltetrahydrofolate synthetase 1 (FTHFS 1) and N^{10}-formyltetrahydrofolate synthetase 2 (FTHFS 2) from the syntrophic acetate oxidizing bacterium, Tepidanaerobacter acetatoxydans Re1, was solved by x-ray crystallography to a resolution of 2.15 Å, and 2.30 Å resolution, respectively. The FTHFS 1 crystal structure has four non-crystallographic related protein molecules in the asymmetric unit of the crystal, while FTHFS 2 has two. The pH optimum in the formylation reaction for FTHFS 1 was determined to be 7.5, while FTHFS 2 had a pH optimum of 9, and it was determined that both enzymes had a temperature optimum of 60°C for their formulation reactions. An attempt to perform the deformylation reaction with both enzymes was unsuccessfully carried out.

Introduction

Background

There is no doubt that fossil fuels are finite energy resources on our planet. Given that "International Energy Outlook 2010" predicts an increase in worldwide energy consumption by 49 % by the end of 2035 (U.S. Energy Information Administration (EIA)), it is obvious that "new" alternative renewable energy sources replacing the fossil based urgently are needed. One such new renewable energy source is biogas, which consists of two major constituents; methane (~60%), which is a major constituent also of natural gas, and carbon dioxide (~40%) (UK'sBiocentre). There are also minor components such as hydrogen sulphide and other constituents in biogas (UK'sBiocentre). Methane gas is energy rich and can be used for generation of heat, electricity and vehicle fuel (UK'sBiocentre). Consequently, the numbers of biogas production plants in Europe are currently increasing (EurObserver), indicative of the growing interest of the biogas as a new renewable energy source.

Biogas is produced naturally in nature during anaerobic microbial degradation of different organic compounds (Schink 1997). A prerequisite for this production is the activity of four physiologically different microorganism groups (figure 1). In the first step of the process, complex organic material such as proteins, polysaccharides, nucleic acids, and lipids are hydrolyzed by the primary fermenting bacteria into oligomers – and monomers, e.g. amino acids, sugars, purines, and fatty acids (Schink 1997). The same bacterial group does in a second step further reduces the monomers by fermentation into more simple compounds such as fatty acids, alcohols, lactate, etc (Schink 1997). Some of the reduced products, for example acetate and hydrogen can be directly converted by the methanogens in the process to methane and carbon dioxide, while other fermented products, such as two – carbon compounds or more, are further degraded by secondary fermenting bacteria to acetate, hydrogen, and carbon dioxide (Schink 1997). These degradation processes represent different anaerobic oxidation reactions (figure 1)

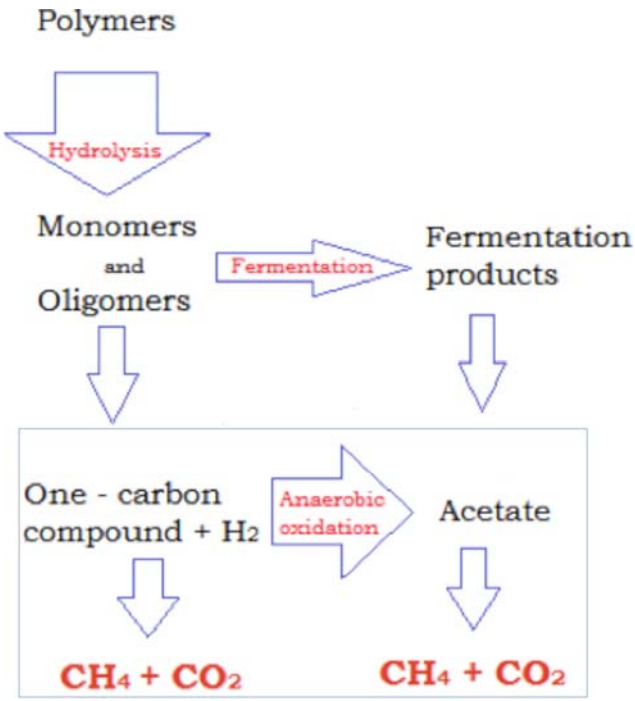

Figure 1. Simplified schedule of the anaerobic degradation of complex organic material in a biogas process. Polymers are firstly hydrolyzed to less complex compound such as oligomers and monomers by primary fermenting bacteria. The same bacterial group further reduces monomers by fermentation into more simple compounds. One-carbon compounds can be directly converted by the methanogens to methane and carbon dioxide, while fermented products, such as two – carbon compounds, are further degraded by secondary fermenting bacteria to acetate, hydrogen, and carbon dioxide (Schink 1997).

In the last step of the anaerobic digestion process, mainly two different methanogenic microorganism groups are active; the hydrogenotrophs, reducing carbon dioxide with hydrogen for the formation of methane; and the acetotrophs that cleas acetate into methane and carbon dioxide (Schink 1997). In addition to these two possible routes, methane can also be produced from acetate via the so-called syntrophic acetate oxidation pathway (Zinder and Koch 1984). Here acetate is first oxidized to hydrogen and carbon dioxide by the syntrophic acetate oxidizing bacteria (SAOB) (Hattori 2008). In a second step hydrogen and carbon dioxide is used by hydrogenotrophic methanogens for the formation of biogas (Zinder and Koch 1984; Jetten et al. 1992; Hattori 2008).

Syntrophic acetate oxidation (SAO) pathway

As mentioned above, methane can be produced from acetate by two different mechanisms (figure 2). In the presence of high ammonia levels, aceticlastic methanogens are inhibited (Schnurer and Nordberg 2008), instead acetate is converted to methane by a two – step mechanism performed by syntrophic acetate oxidizing bacteria (SAOB) in cooperation with hydrogenotrophic methanogens (Schnurer and Nordberg 2008). The high levels of ammonia arise from the degradation of proteins (McCarty 1964) what is a natural occurring process during the biogas production (UK'sBiocentre).

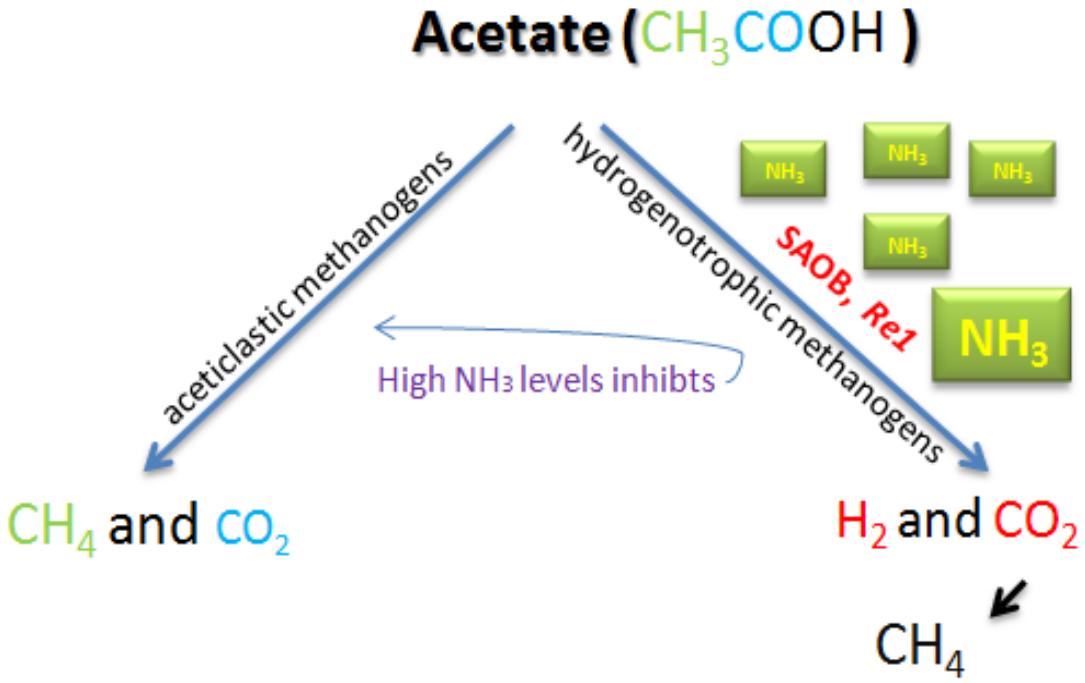

Figure 2. Biogas production from acetate. In the presence of high ammonia levels, the pathway of aceticlastic methanogens are inhibited (Schnurer and Nordberg 2008), instead acetate is converted to methane by a two – step mechanism performed by syntrophic acetate oxidizing bacteria (SAOB), in cooperation with hydrogenotrophic methanogens (reviewed in Hattori 2008).

Syntrophic acetate oxidizing bacteria (SAOB)

The first syntrophically acetate oxidizing bacteria that was isolated was a thermophilic homoacetogen, strain AOR (Acetate-Oxidizing, Rod-shaped bacterium) (Lee and Zinder 1988). Later on several mesophilic: *Clostridium ultunense* (Schnurer et al. 1996), *Syntrophaceticus schinkii* (Westerholm et al. 2010), and thermophilic: *Thermacetogenium phaeum* (Hattori et al. 2000), *Thermatoga lettingae* (Balk et al. 2002), SAOB have been isolated and described. Recently, four new thermo tolerant syntrophically acetate oxidizing bacterium strains Re1, Re2, T1 and T2, all belonging to a novel species *Tepidanaerobacter acetatoxydans,* have been isolated and characterized (Westerholm et al. 2010).

All so far described SAOB, but *Thermatoga lettingae*, are so-called acetogens. Acetogens are a group of phylogenetical diverse bacteria which has in common that they use the so-called Wood-Ljungdahl pathway in the reductive direction producing acetate as the main end product when they grow heterotrophically or autotrophically (Tanner and Woese 1994; Westerholm et al. 2011).

Wood – Ljungdahl pathway (acetyl – coenzyme A pathway)

Wood – Ljungdahl pathway, or as it also called the acetyl – CoA pathway, is a biological process in which carbon dioxide is fixated and synthesized for growth and living in a variety of different bacteria (Ljungdahl 1994; Ragsdale 1997). This makes the Wood – Ljungdahl pathway an important component of the global carbon cycle (Ragsdale and Pierce 2008). The pathway can be summarized in four general steps (figure 3). The first step is the reduction of carbon dioxide (CO_2) to a bound methyl

group [CH_3] in a cascade of reactions, where hydrogen gas is provided via hydrogenase during autotrophic growth (figure 3;1a-e) (Ragsdale and Pierce 2008):

$$CO_2 + 3H_2 + H^+ \longrightarrow [CH_3] + 2H_2O$$

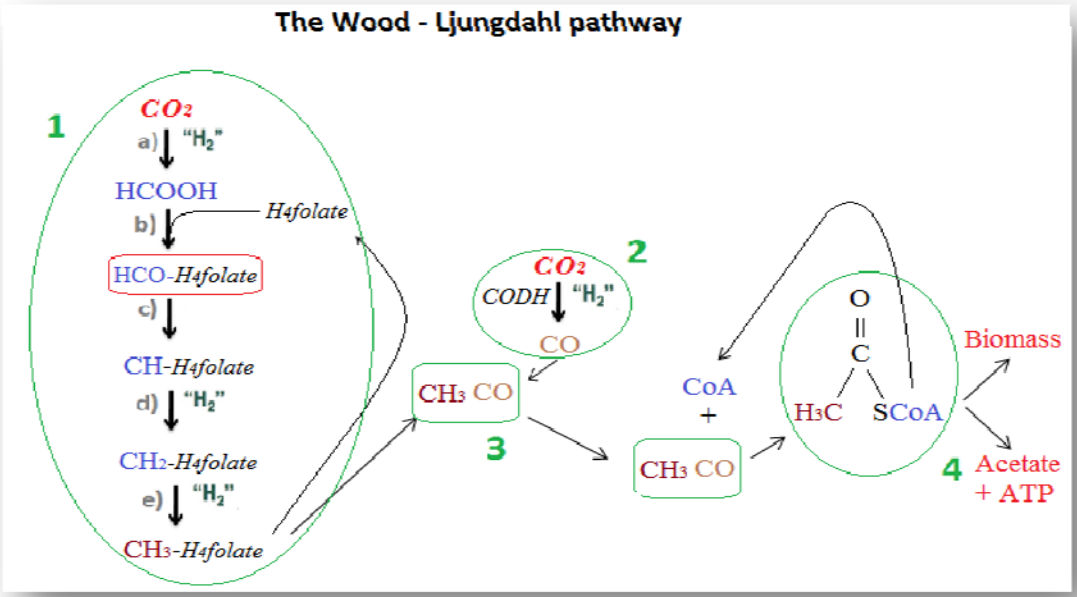

Figure 3. Simplified scheme of the Wood – Ljungdahl pathway and its four general steps. Step 1; The reduction of CO_2 to CH_3 in a series of reaction: a) formate dehydrogenase forms HCOOH, b) the reduction of HCOOH to $HCOH_4$-folate by the H_4-folate in the ATP dependent manner, c) catalyzation of $HCOH_4$-folate to CH^+H_4-folate through the enzyme methenyltetrahydrofolate cyclohydrolase, d) further catalyzation to CH_2H_4folate by the enzyme methylenetetrahydrofolate cyclohydrolase, e) CH_2H_4folate forms CH_3H_4folate with help of methylenetetrahydrofolate reductase. Step 2; The second CO_2 molecule is reduced by CODH to CO. Step 3; The bound CH_3 group and CO together forms CH_3CO. Step 4; ScoA and CH_3CO forms acetyl – CoA by the action of CODH. "H□" means requirement for two electrons and two protons in the reaction (White 1995; Ragsdale and Pierce 2008).

Formate dehydrogenase catalyzes the formation of formate [HCOOH] from carbon dioxide (a) (Ragsdale and Pierce 2008). Formate is then reduced to formyltetrahydrofolate by the coenzyme tetrahydrofolate (H_4-folate) in an ATP dependent reaction (b) (Ragsdale and Pierce 2008). Methenyltetrahydrofolate cyclohydrolase catalyzes the further reaction (c), i.e. the formation of positively charged methenyltetrahydrofolate (CH^+H_4-folate), which later on gets its second proton through the action of methylenetetrahydrofolate (CH_2-H_4folate) cyclohydrolase (d) (Ragsdale and Pierce 2008). Finally, a third proton is taken through the action of methylenetetrahydrofolate reductase (e), which gives a more stable bound of the methyl group to H_4-folate (CH_3-H_4folate) (Ragsdale and Pierce 2008).

During the second step in the pathway, carbon monoxide dehydrogenase (CODH) catalyzes the reaction converting a second carbon dioxide molecule to a carbonyl group, [CO] (Ragsdale and Pierce 2008):

$$CO_2 + H_2 \longrightarrow [CO] + H_2O$$

In the third step, the carbonyl group and the bound methyl group, from the first reaction step, form a bound acetyl, [CH_3CO] (Ragsdale and Pierce 2008):

$$[CO] + [CH_3] \longrightarrow [CH_3CO]$$

The fourth, and the final, step is the reaction of bound acetyl with bound SCoA, which is performed by the enzyme CODH, to produce acetyl – CoA. This product is used as a source for production of acetate and energy (White 1995):

$$[CH_3CO] + [SCoA] \longrightarrow CH_3COSCoA$$

The Wood-Ljungdahl pathway is used by acetogens in the reductive direction for both cell carbon synthesis and for generation of acetyl-CoA, later used for energy conservation. In the same reductive direction this pathway is also used by methanogens, growing on H_2 and CO_2, producing first acetyl–CoA, and later methane for energy conservation (Ragsdale and Pierce 2008). However, there are small differences in Wood-Ljungdahl pathway run by the methanogens and by other bacteria (Ragsdale and Pierce 2008). One of the differences is the enzymatic cofactors which are used by these two prokaryotic subgroups (White 1995).

The Wood-Ljungdahl pathway may also be used by some of the methanogens in the reverse direction, a process called deformylation. In this process CO_2 is produced by the group of methanogens capable of growing on acetate (Ferry 1992). Another group of organisms, sulfate reducing bacteria, can also use the oxidative direction of the Wood-Ljungdahl, generating H_2 and CO_2 from acetate (Ragsdale and Pierce 2008).

Up to date all SAOB, except *T. lettinga*, have been shown to have enzymes activities, or presence of genes encoding enzymes, important for the reactions in the Wood-Ljungdahl pathway. For these organisms, it has been suggested that the mechanism by which acetate is being oxidized to carbon dioxide proceeds through a reverse Wood-Ljungdahl pathway (Hattori 2008). This means that these organisms can operate the pathway in both directions depending on their way of living, i.e. as autotrophs, heterotrophs or as syntrophs (Hattori 2008). This makes them quite fascinating to study. At the time point for this study very little is known regarding the ability of acetogenic strains to use the Wood-Ljungdahl pathway in the oxidative direction during syntrophic growth with hydrogenotrophic methanogens.

Formyltetrahydrofolate synthetase

Tetrahydrofolate (THF or H_4folate) plays a fundamental role in biochemical reactions involved in one carbon unit metabolism of pyrimidines, purines, and amino acids in animals, bacteria and plants (MacKenzie 1984). Formyltetrahydrofolate synthetase catalyzes the activation of formate by THF in an ATP and monovalent cation dependent manner (figure 4) (Rabinowitz and Pricer 1962). In this reaction, monovalent cations, such as K^+ or NH_4^+, play an essential role in binding of the THF to the formate (Rabinowitz and Pricer 1962; Himes and Wilder 1965). Later, for example in acetogens, the product from this reaction, FTHF, is reduced for further synthesis of acetate (figure 3) (Ljungdahl 1986).

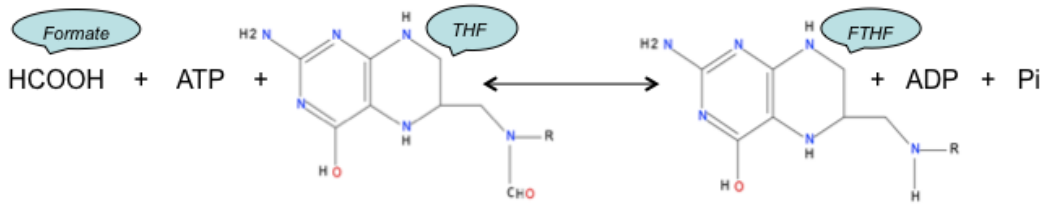

Figure 3. FTHFS catalyzes the reaction of formate and THF in an ATP dependent manner. (Rabinowitz and Pricer 1962)

Acetogens have been suggested to have a bigger number of FTHFS enzyme, compared to methanogens and sulphate reducing bacteria (Ljungdahl 1986). The molecular weight of all studied FTHFS enzymes from bacteria from the genus Clostridia is approximately 240 000 Da (MacKenzie and Rabinowitz 1971). And all of these studied enzymes have four identical substrates binding sites [reviewed in (Himes and Harmony 1973)]. Clostridial FTHFS's have been shown to be catalytically active only in their tetrameric form (Scott and Rabinowitz 1967; Welch et al. 1968). Eukaryotic FTHFS have been shown to be dimeric with three different binding sites, which make these into trifunctional proteins (Paukert et al. 1976; Tan and Mackenzie 1977; Schirch 1978; Hum et al. 1988).

The initial step of the formylation mechanism catalyzed by FTHFS is the reaction of ATP together with formate producing formylphosphate with ADP as a major product (Sly and Stadtman 1963):

ATP + Formate → Formylphosphate + ADP

Structures of FTHFS enzymes

Several structures of FTHFS have previously been solved from different prokaryotic as well eukaryotic organisms. In this study we will describe the biochemical and structural characterization of two prokaryotic FTHFS enzymes. The first successful attempt to get a full nucleotide sequence of a FTHFS enzyme was from *Moorella thermoacetica* (previously called as *Clostridium thermoaceticum*) (Lovell et al. 1990). The investigators of that study managed to get a complete nucleotide sequence of the enzyme and also for a putative ATP binding domain (Lovell et al. 1990). Further crystallographic studies of the same enzyme was partially successful and a structure to 8Å resolution was published (Lewinski et al. 1993). However, a protein structure of the same FTHFS enzyme, solved this time to 2.5Å, together with a deep structural analysis, was presented eight years later (Radfar et al. 2000). In a resent study (Celeste et al. 2012) the putative mechanism of formylation reaction for FTHFS's has been proposed based on ligand-bound structures of a FTHFS. In this study the FTHFS from *M. thermoacetica* was co-crystallized with all potential substrates occurring during the formylation reaction, step by step (Celeste et al. 2012). There is also structural verification of cation binding sites that has been presented for this enzyme (Radfar et al. 2000). The second homologous FTHFS for which the structure was determined was obtained was the FTHFS structure from the hyperthermophilic

bacteria *Thermotoga Maritima,* at 1.85Å resolution (PDB code 3DO6). No publication has yet been published for this FTHFS structure.

X-ray crystallography

Crystallization

Protein crystallization is a science of forcing protein molecules in solution to start attaching to each other in an ordered fashion thus forming solidified macromolecular crystal (McPherson 1999). This may only be overcome by creating a protein supersaturating conditions in the crystallization mixture (McPherson 1999). Such condition starts with a non-equilibrium state, where protein molecules are forced to be in a higher energy state and the only way to decrease that state for them is to start packing together forming aggregates (McPherson 1999). Everything ends with an equilibrium when the macromolecules form crystals (McPherson 1999). Nucleation and growth are two states of crystal formation (McPherson 1999). The first state is characterized by the formation of small, systematically ordered molecular aggregates; and the second state by the accumulation of these molecules together into the solid phase (McPherson 1999). There are many different problems one may encounter during the process off crystallizing protein molecules. One of the biggest problems when crystallizing a biological macro molecule is that there does not exist one solid state in the crystallization medium, there are many (McPherson 1999). Besides forming protein crystals in the supersaturating state, the protein molecules can also form precipitates, oils, and other inorganic molecules in the crystallization drop, such as e.g. salts (McPherson 1999). One of the most important parameters to increase the chances of being successful when crystallizing a protein is the purity of this, since protein molecules have a habit of sticking to other protein molecules (McPherson 1999). There are others factors affecting the crystallization of a protein: the solubility of protein and environmental conditions such as e. g. pH, buffer, precipitants and temperature (McPherson 1999). A crystallization solution, often called a precipitant, may consist of single, or more often, several compounds such as salts, organic solvents, polymers and surfactants. In this study salts, organic solvents and polymers were used as crystallization agents. Surfactants are often used during crystallization of membrane proteins (Bergfors 1999). There are several experimental setups existing when setting up crystallization experiments. The vapor diffusion method is the most common one, followed by the batch method, crystallization by dialysis and the free interface diffusion method (Unge 1999).

X-ray diffraction

A first major step in protein structure determination by x-ray crystallography is to obtain crystals of good enough quality of the studied macro-molecule. The second step is to collect an x-ray diffraction pattern from this crystal. A minor step, which also may affect the results of the determination of proteins three-dimensional structure, is usage of cryo-condition during x-ray diffraction data collection and the use of a cryosolution such as glycerol or a PEG solution to prevent ice formation on the macro-molecule crystal. The cryoprotection is suppose to prevent formation of ice crystals around the protein crystals during the flash freezing of these (Garman 1999). Liquid nitrogen has a temperature of 100 Kelvin (-196 °C). This kind of fast freezing of the crystals is needed to prevent the crystal from being damage during a slow freezing procedure. Keeping the crystal at low temperature such as 100 K is

obligatory to avoid radiation damage of the crystal in the energy rich x-ray beam (Garman 1999). By using different computer programs, as described in materials and methods part, the three-dimensional structure of a protein can, based on the x-ray diffraction dataset collected at a home or a synchrotron x-ray source, be solved, built and refined (Drenth 1994).

Uniqueness of SAOB

Resent studies at the department of Microbiology, SLU, show that the three microorganisms *Tepidanaerobacter acetatoxydans Re1, Syntrophaceticus schinkii,* and *Clostridium ultunense* unlike other acetogens, have two genes encoding for two different FTHFS proteins (unpublished data, personal communication). The fact that these organisms have two FTHFS enzymes is very interesting, considering the fact that the Wood-Ljungdahl pathway is run in the reverse direction by the SAOB during the syntrophic growth [reviewed in (Hattori 2008)]. A tempting hypothesis is that the second FTHFS gene encodes for a FTHFS enzyme that is active in the deformylation reaction.

In a previous bachelor thesis study by the author of this thesis (Roland Bergdahl) the genes coding for FTHFS 1 and FTHFS 2 from *Tepidanaerobacter acetatoxydans Re1* were cloned into a pET15b vector using *Nde*I/*Bam*HI restriction sites. The resulting plasmid vectors were cloned into the *Escherichia coli* protein expression strain BL21 (DE3).

In this study the pH and temperature optimum of the expressed enzymes, FTHFS 1 and FTHFS 2, using different buffer systems in the formylation reaction have been determined. In addition to the biochemical characterizations of the two enzymes the three-dimensional structures of these two enzymes have also been carried out.

Materials and Methods

Cell cultures growth and FTHFS expression

The FTHFS 1 and FTHFS 2 genes, both tagged by 6 His residues at N-terminus, were cloned into a pET15b vector from Novagen and resulting plasmids were transformed into highly competent *Escherichia coli* BL21(DE3) cells as described in a previous bachelor study (data not shown).

Two single *E-coli* BL21 colonies containing the Pet15b vector with either the FTHFS 1 or the FTHFS 2 gene inserted were inoculated into a 5 ml nutritionally rich Lysogeny Broth containing 100 µg/ml ampicillin (LB_{amp}) culture medium in a glass tube. The inoculated culture was incubated for 8 h at 37ºC in a Thermotron incubator shaker (Infors-HT) at 180 rpm. Both colonies were thereafter inoculated into 100 ml LB_{amp}, culture media in a sterile glass flask and pre-cultured over night under the same incubation conditions as the starter culture. These pre-cultures were then used to start the growth of bigger cultures (4 x 700 ml LB_{amp} medium for each FTHFS) in 2 L sterile Erlenmeyer flasks with baffles. Pre cultures were added to the bigger

expression cultures until these had an optical density at a wavelength of 650 nm (OD_{650}) of 0.1. The expression cultures were incubated at the same conditions as the pre cultures were allowed to grow until they had an OD_{650} of 0.5 was reached. Protein expression was then induced by adding Isopropyl β-D-1-thiogalactopyranoside (IPTG) to a final concentration 0.5 mM, the induced expression cultures where then further incubated for 3 hours. The culture media was cooled down for 10 min on ice before harvest of the expressed cells by centrifugation the cultures in 500 ml centrifugation flasks at 8 000 rpm at 4ºC for 10 min. The supernatant was discarded and the remaining cell pellet was frozen at - 20ºC and kept there until further use of the cells.

FTHFS purification and determination

The pellets from the FTHFS 1 and FTHFS 2 cell cultures was thawed on ice for 30 min and re-suspended in 60 ml ice cold 100 mM Tris/HCl pH 7.5 containing 50µg/ml DNase (Sigma) and 2 protease inhibitory tablets (Complete, EDTA free tablets from Roche Diagnostics). Cells were disrupted at 2-bar pressure using one shot model disrupter (Constant Cell Disruption Systems) and centrifuged in 50 ml falcon tubes at 15 000 rpm and at 4ºC to discard pellet. Both 6xHis tagged FTHFS proteins were purified by Immobilized Metal Affinity Chromatography (IMAC) using TALON Metal Affinity Resin (Clontech) according to TALON Metal Affinity Resins User Manual for protein purification (Protocol No. PT1320-1 page 31, Clontech). Equilibration/wash buffer contained 0.05 M Tris pH 7.5 and 0.3 M NaCl. Elution buffer 1 contained 0.3 M NaCl, 0.05 M Tris and 0.15 M imidazole while elution buffer 2 contained 0.3 M NaCl, 0.05 M Tris and 0.3 M imidazole. All three buffers described above also contained protease inhibitory tablets, 1 tablet per 50 ml solution (Roche 2012). The IMAC column contained 20 ml resin corresponding to 90 mg theoretical protein binding. Supernatant was loaded to the IMAC column by the gravity flow method. Then washed with 2 column volumes with washing buffer and the eluates were collected in eppendorf tubes 500 µl x 40 fractions at room temperature. The fractions that contained the protein of interest, as determined by Sodium Dodecyl Sulfate Polyacrylamide Gel Electrophoresis (SDS-PAGE), were pooled together and after imidazole disposal they were stored at - 20ºC

SDS-PAGE analysis and imidazole disposal

All of the collected protein samples from the purification step were characterized by SDS-PAGE. A Precision Plus Protein Dual Color standard ladder (BIO-RAD) was used as molecular weight (MW) reference. Laemmli sample buffer (BIO-RAD) was mixed with beta-mercapto-ethanol (BME) at a volume 95 µl to 5 µl volume and added to the proteins sample 10 µl + 10 µl. This solution was then heated for 5 min at 95°C in a heating block, and thereafter loaded into a pre-cast gel with total amount of 12 µl. The samples were run on a pre-cast 4-15% mini-PROTEAN SDS-PAGE gel (Bio-Rad) for 40 min at a current of 180V, in room temperature. The SDS-PAGE gels were stained by Bio-Safe Coomassie G-250 Stain (BIO-RAD) for 1 h and de-stained in ddH_2O over night. Fractions containing protein of the right size were pooled together and samples were, diluted 1000 times (to remove the imidazole in the samples), and thereafter concentrated again using Vivaspin 20 concentrator column with a 10 000 Dalton MW cutoff (Sartorius Stedim Biotech) at 8°C. Washing buffer consisted of 0.1 M Bis-Tris, 0.15 M NaCl and protease inhibitors.

FTHFS protein concentration determination and mass spectrometry

Protein concentrations were determined by using the manufacturer provided standard assay procedure for 96-wells micro plate by Bio-Rad company (Bio-Rad) The identity of the purified proteins was verified by peptide mapping by mass spectrometry using an Ultraflex MALDI TOF/TOF mass spectrometer (Bruker Daltonics). Peptide mapping was carried out by Åke Engström at the department of medical biochemistry and microbiology, Uppsala University (Biomedical center, Uppsala, Sweden). Dichlorodiphenyltrichloroethane (DTT) was added to samples of purified proteins in following concentrations: 5 mM to FTHFS 2, and 2mM to FTHFS 1 to prevent the proteins from precipitating.

Protein activity assays

Formylation, forward, and deformylation, reverse, FTHFS 1 and FTHFS 2 reaction
All formylation reactions were performed as triplicates and based on the work by Rabinowitz and Pricer, 1962 (Rabinowitz and Pricer 1962). Formylation and deformylation reactions were stopped by adding 0.36 N HCl to the reaction in a 1:2 w:w ratio. Adding HCL also converts the product from 10-formyltetrahydrofolate to 5,10-methenyltetrahydrofolate, which absorbance was spectrophotometrically measured at a wavelength of 350 nm after 10 min using an Infinite M200 plate reader (TECAN).

Effectiveness of beta-mercapto-ethanol (BME) in formylation reactions
Six different concentrations of BME was tested in a one time point assay that contained: 100 mM Na-Formate, 100 mM Bis-Tris/HCl pH 7.5, 10 mM NH_4Cl, (0;5;25;50;100;200) mM BME, protein sample FTHFS 2 = 0.2 mg/ml, and 2 mM Tetrahydrofolate (containing 1 M BME). This mixture was incubated at 37ºC in a water bath for 5 min. The reaction was then started by adding the following mixture: 10 mM $MgCl_2$ and 5 mM ATP, making the total volume of the reaction 100 µl, and the sample was then incubated for 10 min at 37ºC in a water bath before stopping the reaction with 0.36 N HCl.

PH optimum in formylation reactions
Seven different pH values (5/6/7/7.5/8/10) were tested in a one time point assay containing: 100 mM Na-Formate, 100 mM buffer (Sodium citrate/citric acid pH 5 or 6, Tris/HCl pH 7; Bis-Tris/HCl pH 7.5; Bis-Tris propane/NaOH pH 8 or 9, Glycine/NaOH ph 10), 10 mM NH_4Cl, and 2 mM Tetrahydrofolate (containing 1 M BME), 10 mM $MgCl_2$ and 5 mM ATP. This reaction mixture was incubated at 37ºC in a water bath for 5 min. The reaction was started by adding the protein sample (FTHFS 2 = 0.2 mg/ml and FTHFS 1 = 0.0002 mg/ml) making the total volume of the reaction 100 µl, and incubated the sample at 37ºC in a water bath for 10 min at each pH before stopping the reaction with 0.36 N HCl.

PH optimum together with different buffers for the formylation reactions
Three pH values (7/7.5/8) and four different buffers (Bis-Tris propane, HEPES, Bis-Tris, Tricine) using 0.2 mg/ml of FTHFS 2 and three pH values (8.3/8.5/9) and four different buffers (Bis-Tris propane, HEPES, Bicine, Tricine) using 0.0053 mg/ml FTHFS 1 were tested in a one time point assay as described in section “PH optimum in forward reaction.

Temperature optimum for the formylation reactions

Seven different reaction temperatures was tested in a one time point assay containing: 100 mM Na – Formate, 100 mM Bis-Tris/HCl pH 7.5, 10 mM NH_4Cl, and 2 mM Tetrahydrofolate (containing 1 M BME), 10 mM $MgCl_2$ and 5 mM ATP. This mixture was incubated at each temperature tested, 10/20/30/40/50/60/70ºC. The reaction mixture was incubated for 5 min in a water bath and then started by adding protein to the reaction mixture, (FTHFS 2 = 0.2 mg/ml and FTHFS 1 = 0.0002 mg/ml), making the total volume of the reaction 100 µl. The reaction mixture was incubated for 10 min at each temperature before stopping the reaction with 0.36 N HCl.

Protein concentrations dependence in formylation reactions
The time – and protein concentration dependence activity test for the formylation reaction did contain: 100 mM Na-Formate, 100 mM HEPES pH 8.3, 10 mM NH_4Cl, protein sample (FTHFS 2 = 0/0.05/0.85/0.2/0.25/20/50 µg/ml, and FTHFS 1 = 0/0.25/0.35/0.5/5/50 µg/ml), 2 mM Tetrahydrofolate (containing 1 M BME). This mixture was incubated at 60 ºC in a water bath for 5 min. The reaction was started by adding a solution of: 10 mM $MgCl_2$ and 5 mM ATP, making the total volume of the reaction become 100 µl, reactions were stopped with 0.36 N HCl after 1, 2, 3, 4, 5, 10 min.

Deformylation reactions
Deformylation reactions were performed as described by Shoaf and colleagues, 1974 (Shoaf, Neece et al. 1974). The time – and protein concentration dependence activity test for the deformylation reaction did contain: 40 mM Arsenate, 200 mM HEPES pH 8.3, 17 mM cysteine, 20 mM NH_4Cl, protein sample (FTHFS 2 = 10 µg/ml, and FTHFS 1 = 100 µg/ml), 0.7 mM Formyltetrahydrofolate (containing 1 M BME). This mixture was incubated at 37ºC in a water bath for 5 min. The reactions were started by adding a solution of: 30 mM $MgCl_2$ and 2 mM ADP, making the total volume of the reaction 100 µl. The reactions were stopped after 10, 20, 30, 40, 50, 60, 120, 300 and 600 seconds testing FTHFS 2 and after 10, 20, 40, 60, 120, 300 and 600 seconds testing FTHFS 1 at 37 ºC in a water bath by adding 0.36 N HCl.

Protein crystallization
Protein crystallization conditions
Pure samples of recombinantly expressed FTHFS 1 and FTHFS 2 proteins, containing 2 and 5 mM DTT respectively, were concentrated to approximately 6.5 mg/ml using Vivaspin20 concentrator columns with a 10 000 Dalton MW cutoff (Sartorius Stedim Biotech) at 8°C. FTHFS 1 and FTHFS 2 were crystallized by the sitting-drop vapor-diffusion method (Gale R 1993) as following: precipitant – or crystallization solution was added to the wells of a 96 or 24 well micro titer plate. A plastic micro bridge was placed in the well on top of the precipitant, pure protein solution was pipette on top of the plastic bridge. To this protein drop an equal amount of precipitant solution from the well was added. The well with the crystallization drop was closed by putting a siliconized glass cover slip in the cases of the 24 well micro-titer plates and the 96 well plates were sealed with a sealing tape to avoid evaporation.

Initial crystallization experiments for both FTHFS 1, and FTHFS 2 were set up using a (Oryx6) crystallization robot. Initial crystallization conditions for FTHFS 1, and FTHFS 2 was found using the PEG Ion protein crystallization screen (Hampton research). In crystallization experiments with FTHFS 1 small crystals were observed after 3-4 days of incubation. FTHFS 1 was crystallized and the crystallization

condition was optimized by mixing 3 µl protein (7 mg/ml) to 1.5 µl crystallization solution in a sitting drop experiment at 20 ºC. In the bottom of the crystallization well 500 µl of crystallization solution was added, consisting of 0.20 M Sodium-potassium tartrate, 0.10 M Bis-Tris propane pH 6.5 and 18% w/v Polyethylene glycol (PEG) 3350. FTHFS 2 was crystallized and the crystallization condition optimized as described for FTHFS 1, except for that the crystallization solution used was slightly different, containing: 0.24 M sodium-potassium tartrate, 0.12 M Bis-Tris propane pH 6.5 and 16% w/v PEG 3350.

Some crystals from seeding experiment, microseeding (Bergfors 2003), of FTHFS 2 contained: approximately 4 mg/ml pure FTHFS 2 protein solution, pulverized crystalline particles of previously obtained FTHFS 2, 0.2 M K2SO4, 0.1 M ammonium acetate pH 6.8 and 20% w/v PEG 3350 in the 5:2 ratio (2.5 µl protein + 1.0 µl crystallization solution). Seeding procedure was done by the sitting drop vapor diffusion method.

Crystal freezing
Crystals of FTHFS 1 were incubated for a couple of seconds in a cryoprotection solution containing 10% glycerol, 10% ethylene glycol, and 80% crystallization solution prior flash freezing of the crystal in liquid nitrogen. The FTHFS 2 crystals were frozen as described for FTHFS 1 but the crystals where incubated in a cryoprotection solution containing 25% w/v PEG 400 and 75% crystallization solution.

X-ray data collection and process
The X-ray diffraction data sets were collected on FTFHS 1 and 2 crystals using the beamline I911-2 at the Swedish synchrotron radiation laboratory MAX-lab at Lund University, Lund, Sweden. X-ray diffraction data sets from both proteins were processed with the x-ray data processing software, XDS (Kabsch 2010), and integrated data was scaled with the program Scala (Evans 2006), which is part of the CCP4 program suit (CCP4 1994).

Protein structure, homology modeling, structure determination, structure model refinement and sequence alignment

A homology model of FTHFS 2 was made using the I-TASSER structure model prediction server (Zhang 2009) and FTHFS 2 protein sequence. The structure of FTHFS 2 was then solved by molecular replacement methods, using the created homology model as search model, and the molecular replacement program Phaser (McCoy et al. 2007). The structure model was built and manually adjusted using the program Coot (Emsley and Cowtan 2004), and refined with the refinement program Refmac5 (Murshudov et al. 1997) a program in the CCP4 program suit (CCP4 1984). The structure of FTHFS 1 was solved by using a polyAlanin model of the solved FTHFS 2 as molecular replacement search model and by using the same molecular refinement program as for FTHFS 2. Both FTFHS protein models were initially auto built using the auto build function in the program suit PHENIX (Adams et al. 2010). Manual rebuilding and adjustment was performed using the program Coot (Emsley and Cowtan 2004). All structure model cartoon figures were prepared using the protein visualization program, PyMOL (DeLano 2002).

FTHFS 1 and FTHFS 2 sequences were aligned together with most equal protein structure sequence. Clustal Omega (1.0.3) server was used as a multiple sequence alignment program (Sievers et al. 2011).

Results

Expression and purification of the recombinant FTHFS 1 – and FTHFS 2

The recombinant 6xHis-tagged FTHFS 1 and FTHFS 2 proteins, originally cloned from SAOB strain *Tepidanaerobacter acetatoxydans Re1* in a previous study (Roland Bergdahls bachelor thesis), were overexpressed in *E.coli* BL21(DE3), purified by IMAC and analyzed by SDS-PAGE. When these protein samples were analyzed on SDS-PAGE gel clear visible monomers of FTHFS 1, lane 2-15 (figure 6), and of FTHFS 2, lane 6-15 (figure 7), were seen. Both proteins have an estimated molecular weight of 60 kDa, indicated in figure 6 with an arrow.

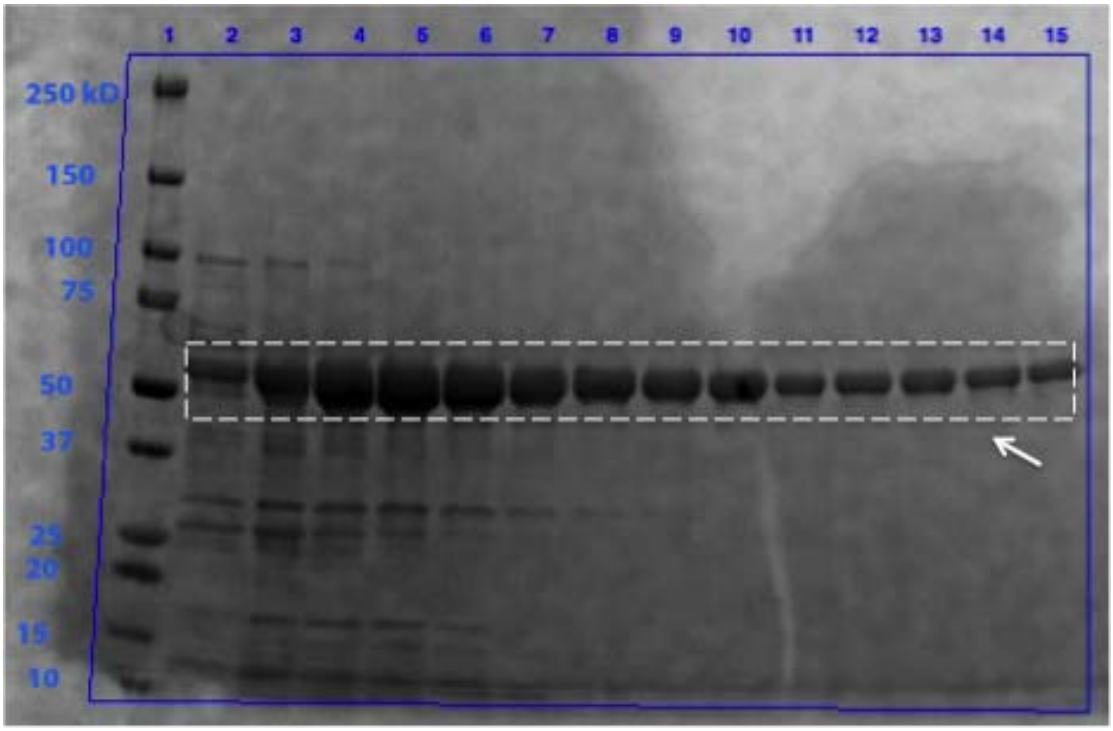

Figure 6. SDS-PAGE analysis of purified eluted fractions contained FTHFS 1 protein. Pre-cast 4-15% SDS-PAGE analysis of the amounts of purified by IMAC 6xHis–tagged FTHFS 1 fractions. Lane 1: MW ladder. Lane 2-15: pure 6xHis-tagged FTHFS 1 overexpressed in *E.coli* BL21(DE3), shown with an arrow.

One purified band of each protein was then analyzed by mass spectrometry and identified as FTHFS 1 and FTHFS 2 respectively (data not shown). Purified fractions containing proteins of right size were pooled together and diluted 1000 times in order to remove imidazole, using concentrator tube with a 10k Dalton MW cutoff. Imidazole was removed as it may disturb protein activity measurements and

crystallization experiments. Later, the BIO-RAD protein assay was used to determine the concentration of both proteins.

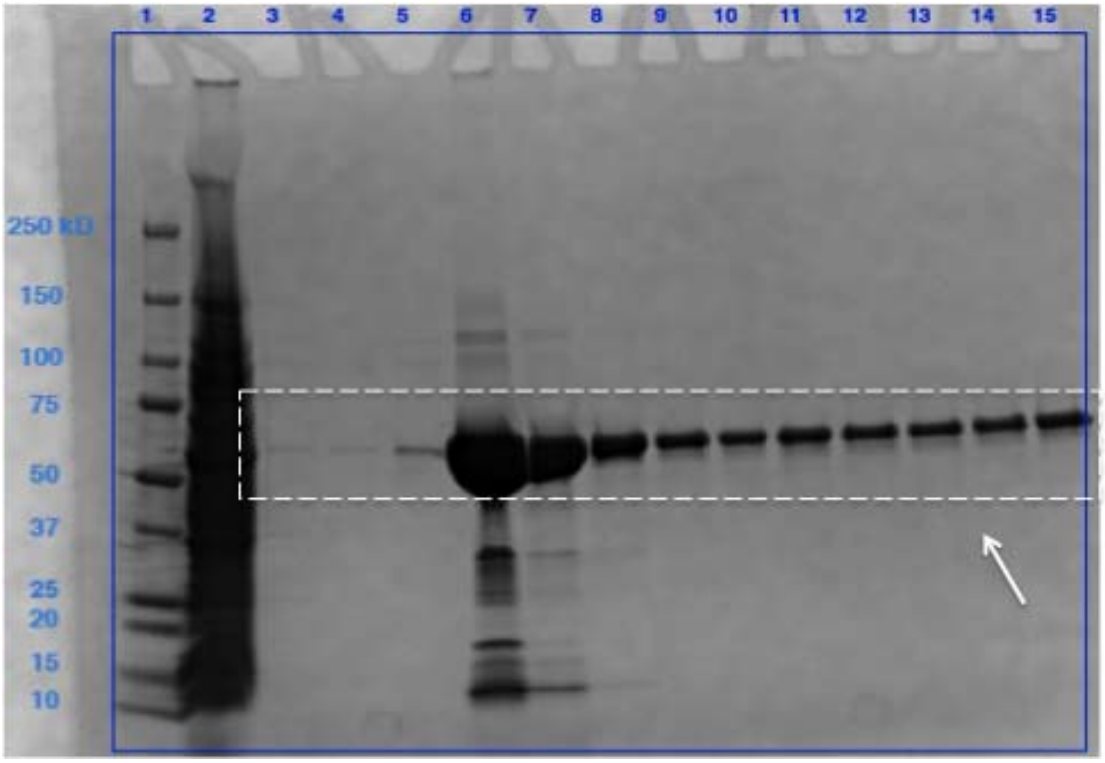

Figure 7. SDS-PAGE analysis of bacterial cell lysate and purified eluted fractions containing FTHFS 2 protein monomers. Pre-cast 4-15% SDS-PAGE analysis of the amounts of purified 6xHis–tagged FTHFS 2 fractions from IMAC. Lane 1: MW ladder. Lane 2: unbound cell lysate from IMAC purification column. Lane 3: washing step. Lane 4-5: elution fractions nr 4 and 5 respectively. Lane 6-15: pure 6xHis-tagged FTHFS 2 overexpressed in *E.coli* BL21(DE3), shown with an arrow.

Proteins activity measurements

Enzymatic activity experiments for both proteins were analyzed by measuring the absorbance at 350 nm for both formylation and deformylation reactions.

Formylation reaction

Beta-mercapto-ethanol (BME) effectiveness test, pH and temperature optimum were analyzed in formylation reactions using FTHFS 1 and FTHFS 2 enzymes. First the effect of BME on the formylation reaction catalyzed by FTHFS 2 (figure 8) was tested. The same experiment was also performed on the FTHFS 1 enzyme (data not shown). Both experiments clearly indicated that BME was not needed for the enzyme activity; therefore no BME was added to the formylation experiments.

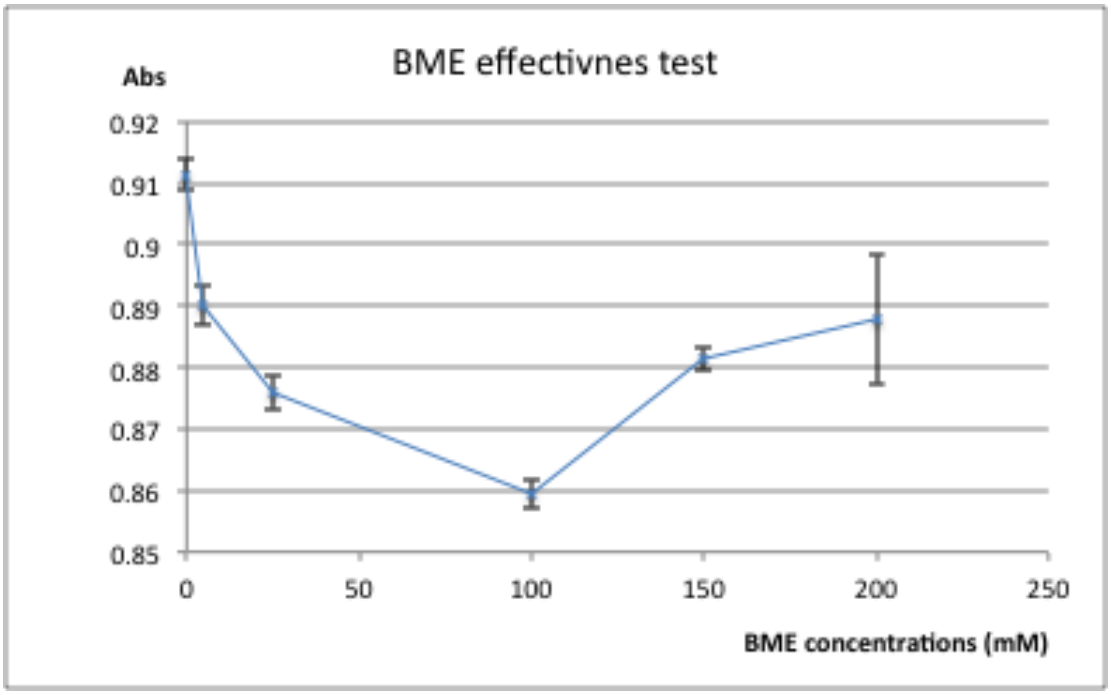

Figure 8. BME effectiveness analysis on formylation reaction catalyzed by FTHFS 2. Enzymatic formylation reaction catalyzed by FTHFS 2 using different concentrations of BME for 10 min during incubation at 37ºC. By measuring the increase of the product at 350 nm, the changes in absorbance values were recorded and shown in triplicates representing the standard error of the mean (SEM).

For FTHFS 1 and FTHFS 2, the analysis was performed at seven different pH values ranging from pH 5 to 10 (figure 9 and 10). The pH optimum test revealed that FTHFS 1 was most active at a pH value of approximately 9 and the FTHFS 2 at a pH value of 7.5.

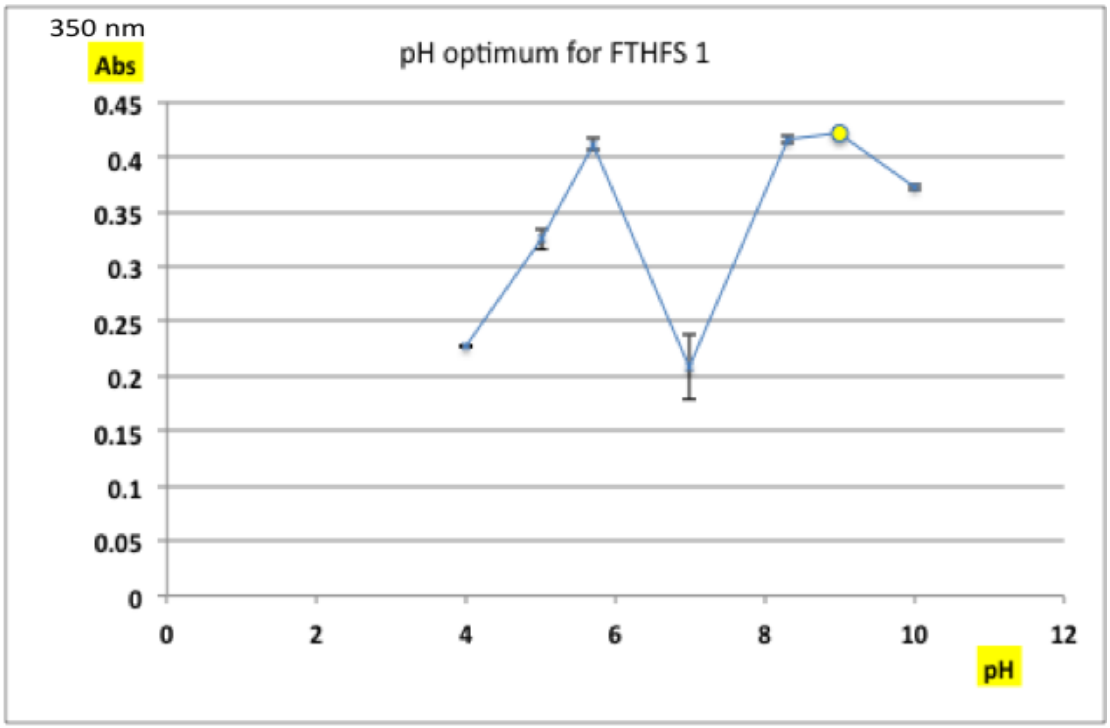

Figure 9. Determination of pH optimum of the FTHFS 1. Formylation reaction was catalyzed by FTHFS 1 under seven different pH values for 10 min during incubation at 37ºC. All of the buffer systems were in final concentration of 100 mM. Sodium citrate/citric acid (pH 5 and 6), Tris/HCl (pH 7), Bis-Tris/HCl (pH 7.5), Bis-Tris propane/NaOH (pH 8 and 9), Glycine/NaOH (ph 10) were used as buffer systems. By measuring the increase of the product at 350 nm, the changes in absorbance values were recorded and shown in triplicates representing the standard error of the mean (SEM).

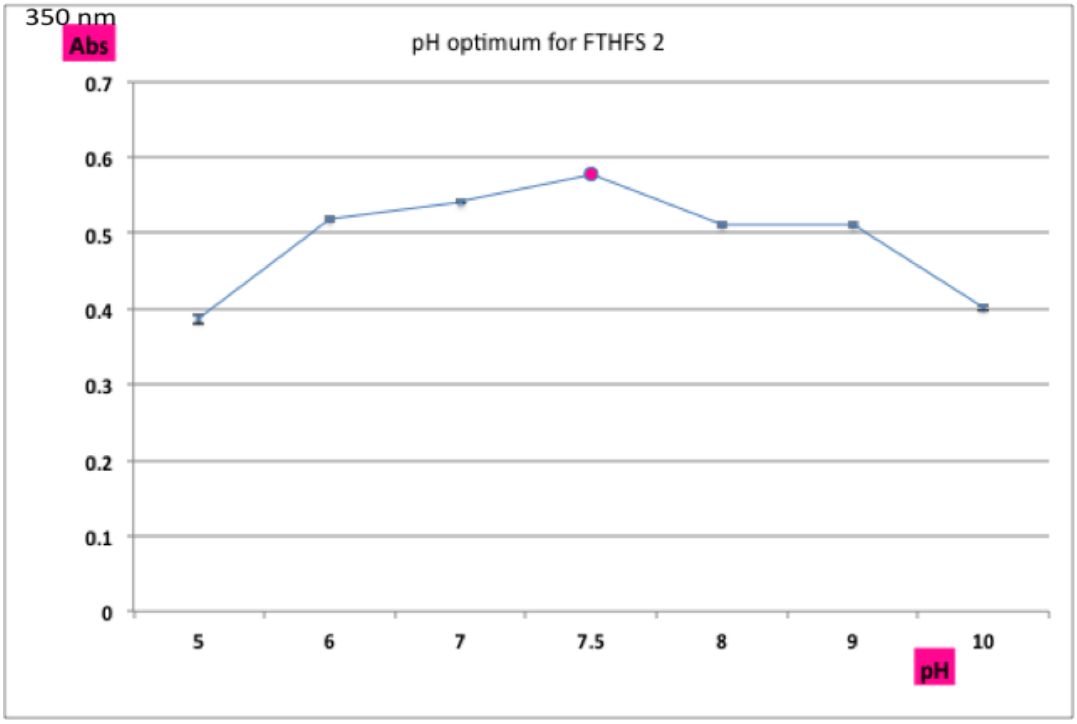

Figure 10. Determination of pH optimum of the FTHFS 2. Formylation reaction was catalyzed FTHFS 2 under seven different pH conditions for 10 min during incubation at 37ºC. All of the buffer systems were in final concentration of 100 mM. Sodium citrate/citric acid (pH 5) and 6, Tris/HCl (pH 7), Bis-Tris/HCl (pH 7.5), Bis-Tris propane/NaOH (pH 8 and 9), Glycine/NaOH (ph 10) were used as buffer systems. By measuring the increase of the product at 350 nm, the changes in absorbance values were recorded and shown in triplicates representing the standard error of the mean (SEM).

The effect of temperature on the activity of FTHFS 1 and FTHFS 2 enzymes illustrated that both enzymes were active at mesophilic as well as at thermophilic temperatures (figure 11 and 12). However, both enzymes catalyzed both substrates most effectively at 60^0C.

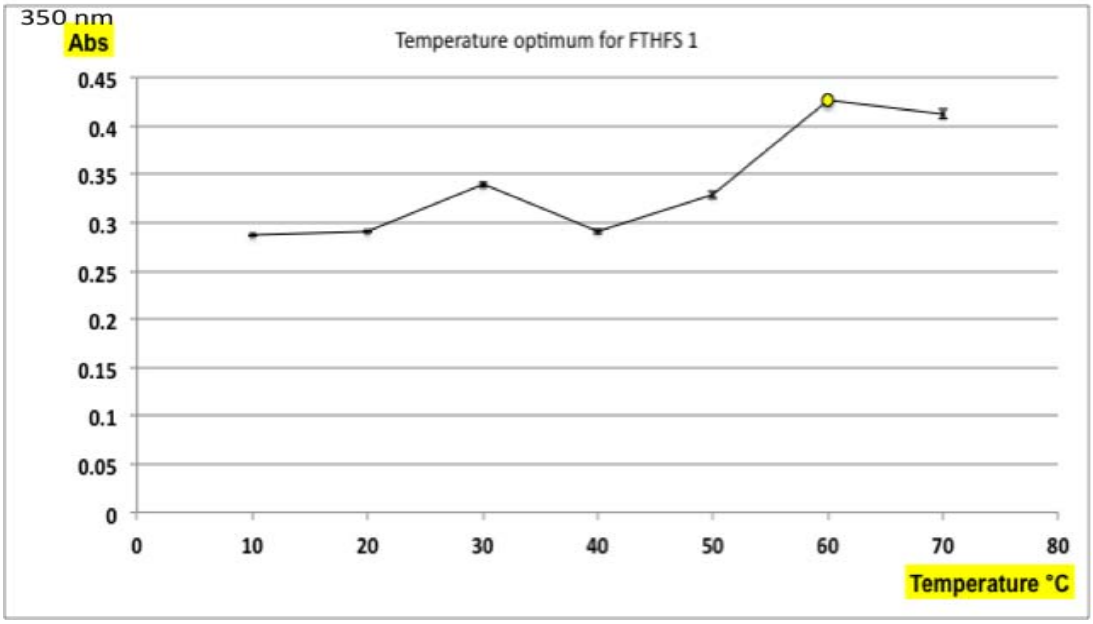

Figure 11. Determination of temperature optimum of the FTHFS 1. Formylation reaction was catalyzed FTHFS 1 under seven different temperature conditions for 10 min of incubation at 37ºC. HEPES at 100 mM final concentration, pH 8.3, was used as buffer system. By measuring the increase of the product at 350 nm, the changes in absorbance values were recorded and shown in triplicates representing the standard error of the mean (SEM).

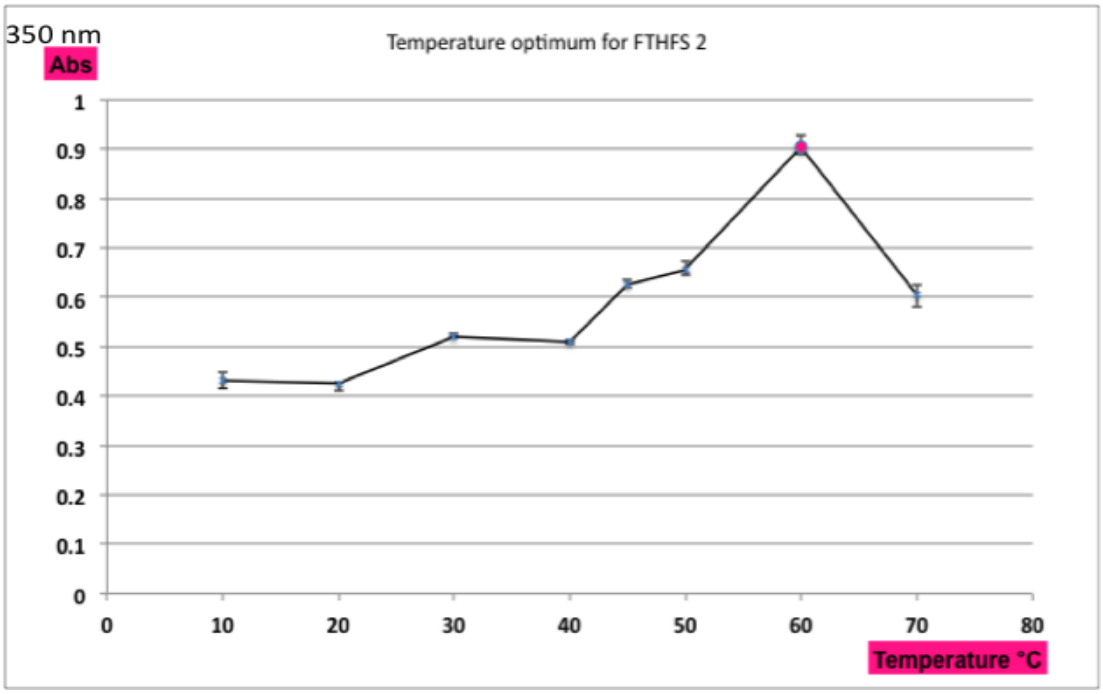

Figure 12. Determination of temperature optimum of the FTHFS 2. Formylation reaction was catalyzed FTHFS 2 under seven different temperature conditions for 10 min of incubation at 37ºC. HEPES at 100 mM final concentration, pH 8.3, was used as buffer system. By measuring the increase of the product at 350 nm, the changes in absorbance values were recorded and shown in triplicates representing the standard error of the mean (SEM).

Six different protein concentrations were used for both FTHFS 1 (figure 13) and FTHFS 2 (figure 14). The most constant increase in activity rate by time was seen at concentration of 0.35 µg/ml and 0.25 µg/ml for FTHFS 1 and FTHFS 2, respectively.

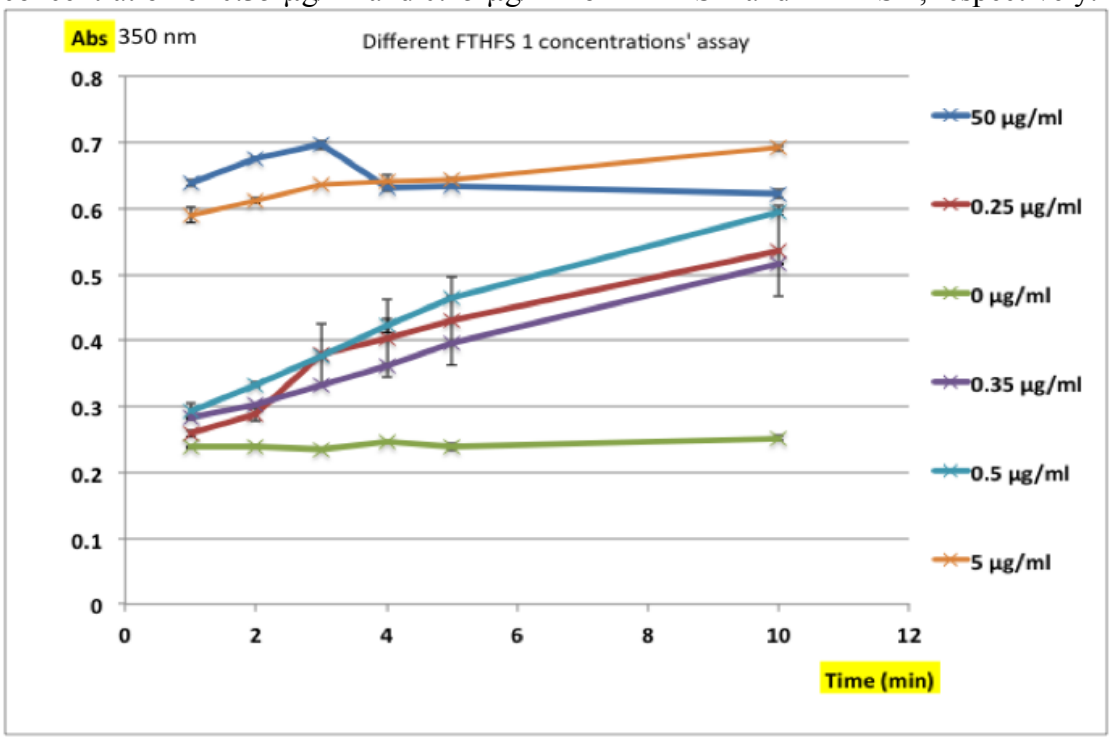

Figure 13. Enzymatic analysis of different FTHFS 1 concentrations. FTHFS 1 catalyzes the formylation reaction using six different concentrations during 1, 2, 3, 4, 5 and 10 min of time at 60ºC. HEPES at 100 mM final concentration, pH 8.3, was used as buffer system. By measuring the increase of the product at 350 nm, the changes in absorbance values at each minute were recorded and shown in triplicates representing the standard error of the mean (SEM).

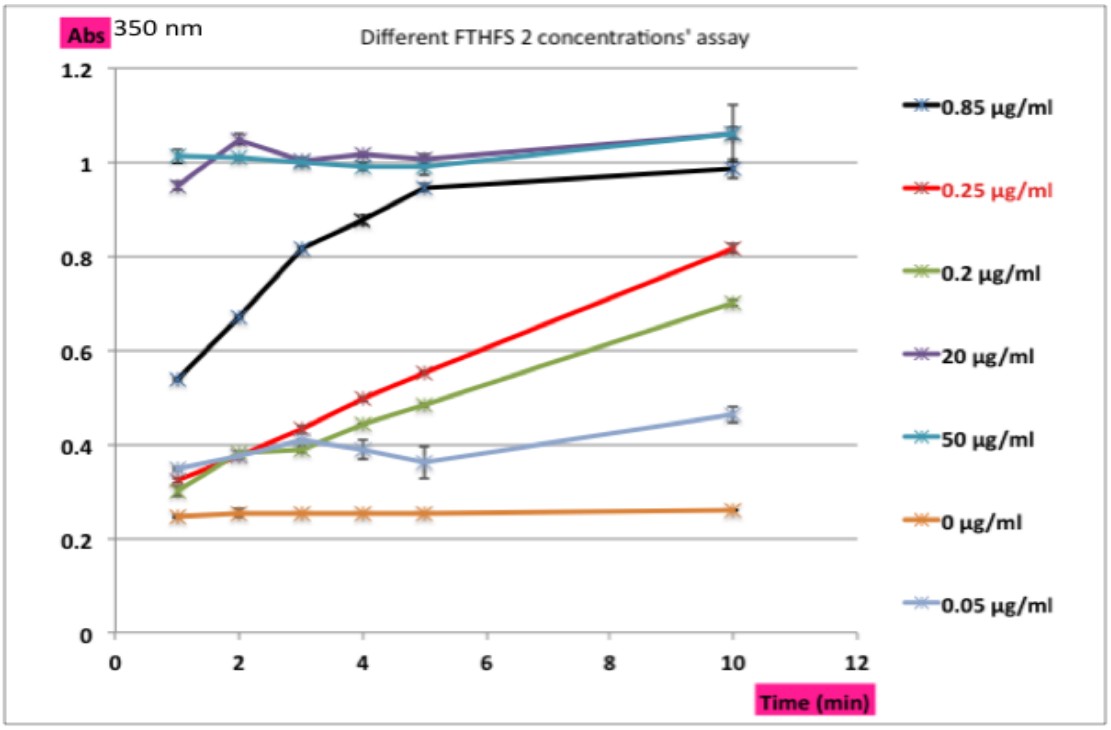

Figure 14. Enzymatic analysis of different FTHFS 2 concentrations. FTHFS 2 catalyzes the formylation reaction using six different concentrations during 1, 2, 3, 4, 5 and 10 min of time at 60ºC. HEPES at 100 mM final concentration, pH 8.3, was used as buffer system. By measuring the increase of the product at 350 nm, the changes in absorbance values at each minute were recorded and shown in triplicates representing the standard error of the mean (SEM).

Different buffer systems and different pH values of these were tested during formylation reaction. The optimal buffer system at 60ºC, of the ones that were tested, for FTHFS 1 was found to be Tricine at 100 mM final concentration with a pH of 9 (Table 2) and the best for FTHFS 2 was HEPES at 100 mM final concentration with a pH of 7.5 (Table 1).

Table 1. Buffer – and its pH values analysis during FTHFS 2 enzymatic activity. Different buffers with pH values (as given in table) were tested in formylation reaction catalyzed by FTHFS 2 for 10 min of incubation at 37ºC. By measuring the increase of the product at 350 nm, the changes in absorbance were recorded. The experiment was run 3 times with the same results.

Buffer system and used pH	Absorbance of enzymatic activity of FTHFS 2
Bis-Tris propane pH7	0.81
Bis Tris propane pH7.5	0.83
Bis Tris Propane pH8	0.86
HEPES pH7	0.88
HEPES pH7.5	0.89
HEPES pH8	0.85
Tricine pH7.5	0.71
Tricine pH8	0.54
Bis-tris pH7.5	0.84

Table 2. Buffer – and its pH values analysis during FTHFS 1 enzymatic activity. Different buffers with pH values (as indicated in table) were tested in formylation reaction catalyzed by FTHFS 1 for 10 min of incubation at 37ºC. By measuring the increase of the product at 350 nm, the changes in absorbance were recorded. The experiment was run 3 times with the same results.

Buffer system and used pH	Absorbance of enzymatic activity of FTHFS 1
HEPES pH 8.3 60C	0.61
Bis tris propane pH 9 60C	0.60
Tricine pH 8.3 60C	0.71
Tricine pH 9 60C	0.72
Bicine pH 9 60C	0.59
Bicine pH 8.5 60C	0.56
Bis tris propane pH 8.3 60C	0.602

Deformylation reaction

The time dependence activity test for the deformylation reaction was performed with FTHFS 2 (figure 15) and FTHFS 1 (figure 16). The absorbance was measured at 0, 10, 20, 30 (not in FTHFS 1 case), 40, 50 (not in FTHFS 1 case), 60, 120, 300 and 600 seconds.

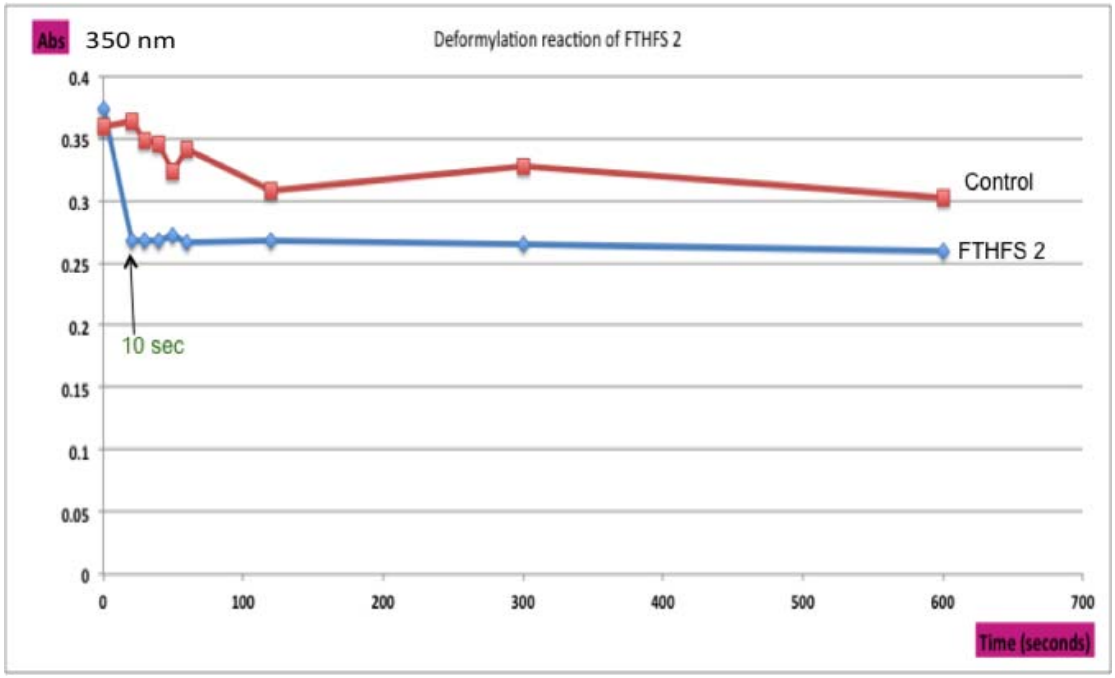

Figure 15. Deformylation reaction catalyzed by FTHFS 2. The samples were analyzed after 0, 10, 20, 30, 40, 50, 60, 120, 300 and 600 seconds of incubation at 37ºC. HEPES at pH 8.3 were used as buffer system. By measuring the disappearance of the product at 350 nm, the changes in absorbance values at each time point were recorded and shown in one single experiment.

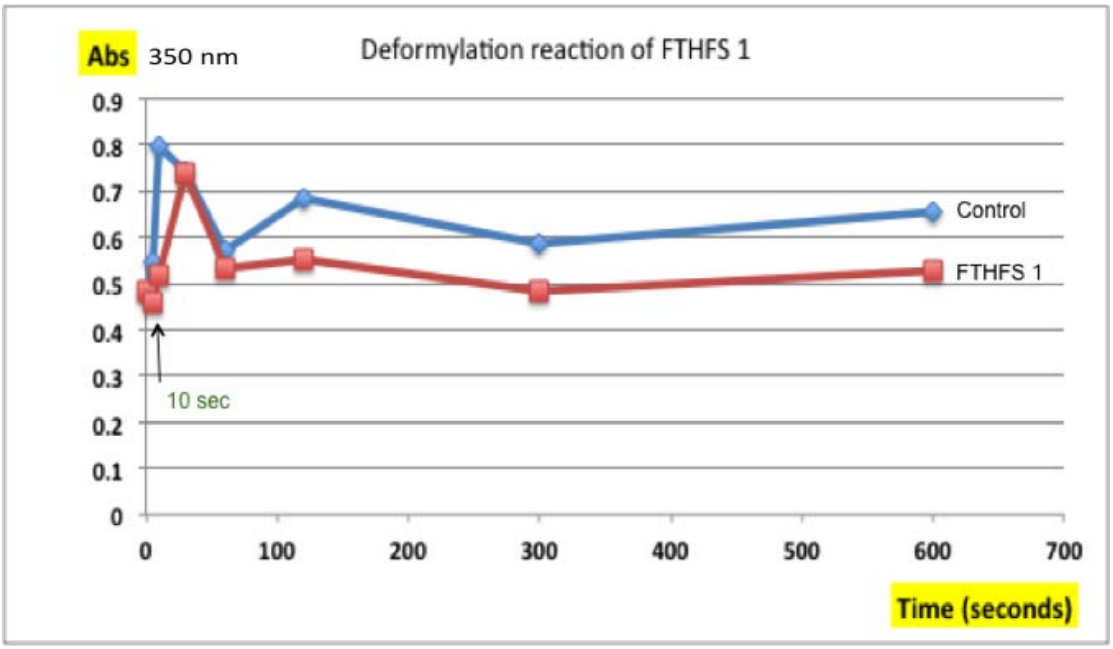

Figure 16. Deformylation reaction catalyzed by FTHFS 1. The samples were analyzed after 0. 10, 20, 40, 60, 120, 300 and 600 seconds of incubation at 37ºC. HEPES at 100 mM final concentration, pH 8.3, was used as buffer system. By measuring the disappearance of the product at 350 nm, the changes in absorbance values at each time point were recorded and shown in one single experiment.

Crystallization

The FTHFS 1 optimized crystals that were used for X-ray diffraction data collection had the following crystallization conditions: 6.5 mg/ml protein, 0.20 M Sodium-potassium tartrate, 0.10 M Bis-Tris propane pH 6.5, 18% w/v Polyethylene glycol (PEG) 3350. The FTHFS 2 crystals were crystallized using: 0.24 M Sodium-potassium tartrate, 0.12 M Bis-Tris propane pH 6.5, 16% w/v PEG 3350. The crystals of FTHFS 1 and FTHFS 2, grown using the above-described conditions had a very similar morphology (figure 17:B). The crystals appeared after 16 hours, and had the shape of a sward edge. The crystals of FTHFS 2 was obtained by seeding under other conditions; approximately 4 mg/ml pure FTHFS 2 protein solution, seeds of previously obtained FTHFS 2, 0.2 M K2SO4, 0.1 M ammonium acetate pH 6.8 and 20% w/v PEG 3350. These crystals appeared after 1-2 weeks and had a very homologous and proportioned shape of a square or a rod with fine sharp ends (figure (17:A).

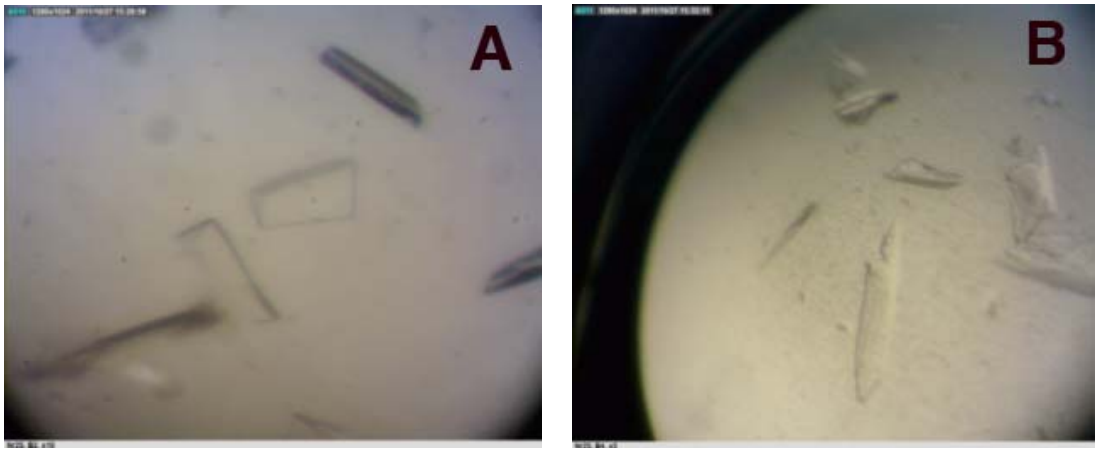

Figure 17. FTHFS 1 and FTHFS 2 crystals. Figure A shows a representative picture of FTHFS 2 crystals. These crystals were obtained by seeding, and by mixing 4 mg/ml pure FTHFS 2 together with pulverized crystalline particles of a previously obtained FTHFS 2 crystal. Initialy FTHFS 2 was crystallized by the sitting drop vapor diffusion method by mixing 0.2 M K_2SO_4, 0.1 M ammonium acetate pH 6.8 and 20% w/v PEG 3350 and protein solution in a 5:2 ratio (2.5 µl protein + 1.0 µl crystallization solution). FTHFS 2 Crystals appeared after 1-2 weeks incubation of the crystallization experiments. Figure B shows a representative picture of FTHFS 2 and FTHFS 1 crystals. 6.5 mg/ml pure FTHFS 1 and FTHFS 2 samples were crystallized by the sitting drop vapor diffusion method. FTHFS 1 crystallized with 0.20 M Sodium-potassium tartrate, 0.10 M Bis-Tris propane pH 6.5, 18% w/v PEG 3350 and FTHFS 2 crystallized with 0.24 M Sodium-potassium tartrate, 0.12 M Bis-Tris propane pH 6.5, 16% w/v PEG 3350. Crystals emerged after approximately 16 hours.

X-ray diffraction data collection and processing

Crystals of FTHFS 1 that gave useful X-ray diffraction data sets were soaked in a cryo solutions containing 10% glycerol, 10% ethylene glycol, and 80% crystallization solution prior flash freezing the crystals in liquid nitrogen. The FTHFS 2 crystals were soaked in: 25% w/v PEG 400 and 75% crystallization solution. The data collection, refinement and the final model statistics are presented in table 3.

Table 3. Data collection, processing and refinement statistics

Statistics	**FTHFS 1**	**FTHFS 2**
Beamline[a]	I911-2	I911-2
Wavelength (Å)	1.04088	1.04088
No. Of images	512	360
Oscillation range	0.25	0.5
Space group	$P2_12_12_1$	C2
Cell Parameters		
a (Å)	90.04	113.04
b (Å)	100.98	98.12
c (Å)	258.05	108.76
b(Å)		101.51
Resolution range	29.60-2.15	29.64-2.42
No. Of observed reflections	677507	195552

No. Of unique reflections	126940	50934
Average multiplicity	5.3	3.8
Completness (%)	98.9	98.5
Rmerge[c] (%)	7.1 (53.2)[b]	4.8 (43.6)[b]
Rmeas	7.8 (58.7)[b]	5.6 (50.6)[b]
I/sigI	20.0 (3.8)[b]	15.4 (2.8)[b]
R[d]/Rfree (%)	21.5/25.2	23.3/28.8
Average Bfactor	30.836	47.715
Bond lengths (Å)	0.008	0.01
Bond angles (deg.)	1.064	1.243
Protein molecules	4	2
No. residues in protein	2207	1088
Ramachandran outliers (%)	0.4	0.3

[a]Beamline at MAX-lab, Lund, Sweden
[b]Numbers in parentheses are for the highest resolution bins
[c]$R_{merge} = \Sigma_{hkl} \Sigma_i | I - < I > | / \Sigma_{hkl} \Sigma_i | I |$
[d]$R = \Sigma | |F_o| - |Fc| | / \Sigma |F_o|$; the final R-factor is given

FHTFS 1 structure

The structure of FTHFS 1 was solved by molecular replacement methods, and the structure was refined to 2.15Å resolution with a final R and R_{free} value of 21.5% and 25.2%, respectively. There are four non-crystallographic symmetry (NCS) related FTHFS 1 protein molecules in the asymmetric unit of the crystal (figure 18). The tetrameric FTHFS 1 is arranged by two 2-fold and one 4-fold NCS symmetry in the asymmetric unit. All seven-cysteine residues in the protein molecule were found to be free and did not take part in forming any disulfide bridges in the protein.

The electron density for FTHFS 1 was found to be continuous for most of the amino acids in the protein, especially in NCS chain A. Only the first three side chain residues in chain A were lacking electron density, however the density of the backbone in this region was acceptable. NCS chain B had the same good electron density as for chain A, except for residue 71. The quality of the electron density for a big part of the chains C and D were clearly lower than for the chains A and B. In chain C no electron density was found for the following residues: 1-3, 69-71, 559; and in chain D: 1-3, 69-71,553-559. This might also explains the higher value of refined temperature factors in these two chains compared with the other two.

One mutation was found in the FTHFS 1 structure compared with the deposited amino acid sequence for the enzyme. A threonine had been mutated to an alanine at position 377 compared with the native sequence. This has also been confirmed by sequencing the gene. The electron density for an alanine in the structure is clearly seen instead of a threonine. This mutation probably appeared during the PCR amplifications of the FTHFS 1 gene just before cloning procedure.

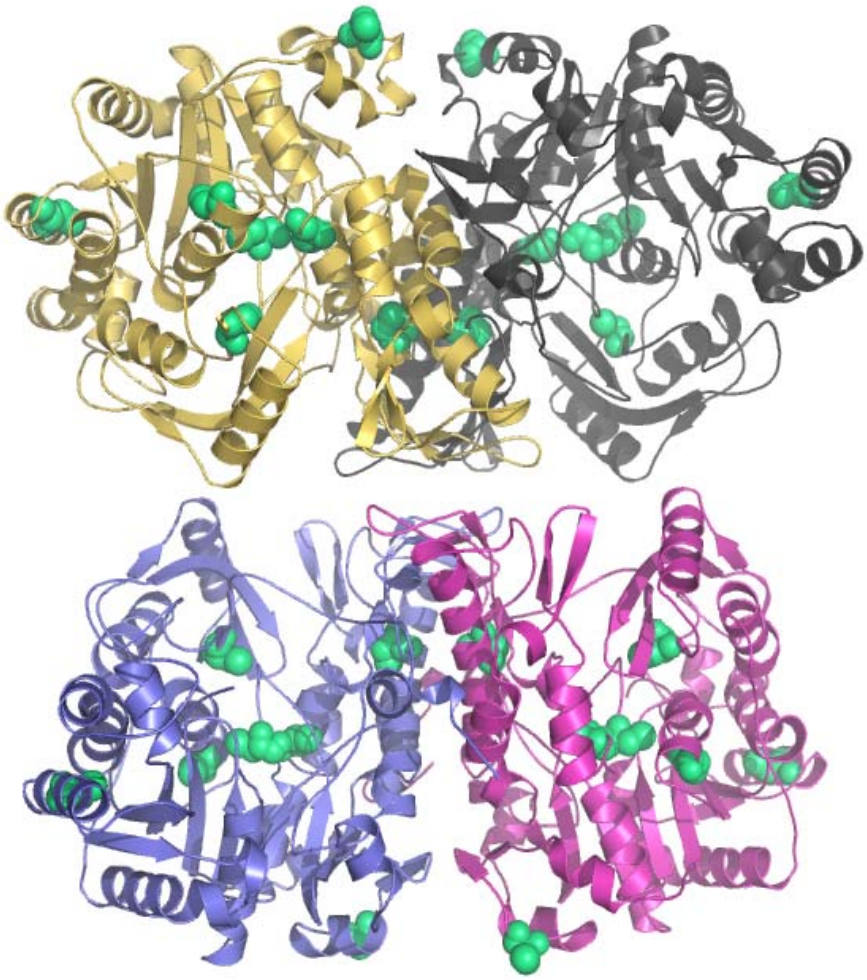

Figure 18. Cartoon representation of the four NCS related molecules of the FTHFS 1 structure, depicted in yellow, gray, blu and purple. All of the free cysteine residues of the four NCS molecules are depicted as green spheres.

FHTFS 2 structure

The structure of the FTHFS 2 was solved by molecular replacement methods and refined to 2.3Å resolution with a final R and Rfree value of 23.3% and 28.8% respectively. The FTHFS 2 structure model has two NCS-related protein molecules in the asymmetric unit of the crystal forming a structural dimer (figure 19). Dimeric FTHFS 2 was arranged by one 2-fold noncrystallographic symmetry in the asymmetric unit. All six-cysteine residues of the protein were readily identified in the protein structure and none of the cysteine residues did take part in forming a disulfide bridge.

The electron density for FTHFS 2 was found to be continuous for most of the amino acids and both FTHFS 2 NCS chains in the structure had similar refined temperature factors. The following residues in either of the two NCS chains of the structure are either missing or have bad electron density: 1-3, 48-53, 342-344, and 430-437. One of the cysteine residues was located in the region without density and that is why this residue is missing in figure 19.

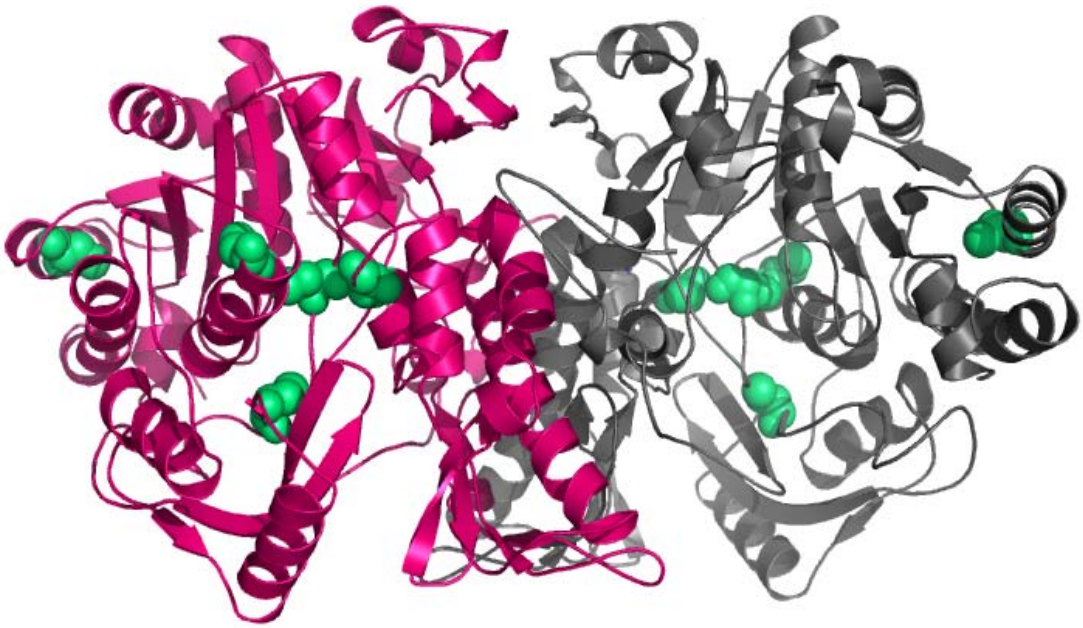

Figure 19. Cartoon representation of the two NCS related molecules of the FTHFS 2 structure, depicted in purple and gray, and with all cysteine residues depicted as a green spheres. One cysteine in each monomer is absent because of the missing electron density in this region.

Sequence alignment

Multiple sequence alignment was carried out with FTHFS 1, FTHFS 2 and the most related sequence belonging to *M. thermoacetica,* PDB code 1EG7 (figure 20). Conserved residues among compared protein sequences are marked with a star I the alignment (*) and those identical in ATP binding proteins are marked in red. The sequence identity between FTHFS 1 and FTHFS 2 is 73%; the sequence identity between FTHFS 1 and FTHFS from *M. thermoacetica* is 69%; between FTHFS 2 and FTHFS *M.thermoacetica* it is 64%.

```
FTHFS_1          -MSYKSDIEIAQEAKIEHIKDVATKIGLCEDDIEYYGKYKAKIDYNLLKRFEDKKDAKLI
FTHFS_2          -MTFKSDIEIAQSVKLQDIREIAAKLGLTEDDIDLYGKYKAKVDYNLLNNCNG-KKAKLI
FTHFS_M.TH.      MSKVPSDIEIAQAAKMKPVMELARGLGIQEDEVELYGKYKAKISLDVYRRLKDKPDGKLI
                      *******  *       *   *  **    *******              ***

FTHFS_1          LTTAINPTPAGEGKTTTTVGLGDALRRLGKNAMIALREPSLGPVFGIKGGAAGGGYAQVV
FTHFS_2          LTTAITPTPAGEGKTTTTIGAADALTRLGKKTIVALREPSLGPVFGIKGGAAGGGYAQVV
FTHFS_M.TH.      LVTAITPTPAGEGKTTTSVGLTDALARLGKRVMVCLREPSLGPSFGIKGGAAGGGYAQVV
                 * *** ***********  *  *** ****     ******** ****************

FTHFS_1          PMEDINLHFTGDFHAIGAANNLLAAMIDNHIYQGNELNIDPRRITWKRCVDMNDRQLRFV
FTHFS_2          PMEDINLHFTGDIHAITAANNLLAAMVDNHIFQGNQLNIDTRRVVWRRAVDINDRQLRFV
FTHFS_M.TH.      PMEDINLHFTGDIHAVTYAHNLLAAMVDNHLQQGNVLNIDPRTITWRRVIDLNERALRNI
                 ************ **   * ****** ***  *** **** *   * *  * * * **

FTHFS_1          VDGLGGKANGTPREDGYDITVASEIMAVFCLANDMEDLKNRLARIIIGYTYDGKPVTAGQ
FTHFS_2          IDGLGGKANGVPREDGFDITVASEVMAIFCLANDIMDLKERLAKIVVAYDREGKPVTAGD
FTHFS_M.TH.      VIGLGGKANGVPRETGFDISVASEVMACLCLASDLMDLKERFSRKVVGYTYDGKPVTAGD
                   ******** *** * ** **** **  *** *  *** *       *   *******

FTHFS_1          LKAQGAMAALLKDAFKPNLVQTLEGTPAFVHGGPFANIAHGCNSIIATKMALKLADYVVT
FTHFS_2          LKAQGAMAALLKDALKPNLVQTLEGTPAFVXGXPFXXIAHGCNSVIATKMAMHLADYVVT
FTHFS_M.TH.      LEAQGSMALLMKDAIKPNLVQTLENTPAFIHGGPFANIAHGCNSIIATKTALKLADYVVT
```

```
                 * *** ** * *** ********* ****  * **  ******* **** *  *******

FTHFS_1          EAGFGADLGAEKFLDIKCRMADIRPDAVVIVATIRALKYNGGVKKEDLNQENLDALKKGL
FTHFS_2          EAGFGADLGAEKFIDIKCRLAGLKPDATVIIVATVRALKYNGGLAKADLEKEDLNALAKGI
FTHFS_M.TH.      EAGFGADLGAEKFYDVKCRYAGFKPDATVIVATVRALKMHGGVPKSDLATENLEALREGF
                 ************* * *** *   ***  **** ****  **  * **  * * **  *

FTHFS_1          PNLLKHVENITEKYGIPAVVAINQFPTDTERELALVQEECNRLGVNAVLSEVWAKGGEGG
FTHFS_2          PNLLKHVENITQVFKLPAVVAINRFPQDTEAELKLVEDRCNELGVNVALSEVWAKGGEGG
FTHFS_M.TH.      ANLEKHIENIG-KFGVPAVVAINAFPTDTEAELNLLYELCAKAGAEVAL--SWAKGGEGG
                  ** ** ***      ******* ** *** ** *    *   *    *   ********

FTHFS_1          LELAKEVVRIIEEGKN---NFKPIYDLDMGIADKITTIAKEIYGADGVEFAPAALKEINT
FTHFS_2          IALAEELIRLTEDNKASNKGLAYVYELDMPIEEKIRAISQKIYGADDVMFTDKALKEIAN
FTHFS_M.TH.      LELARKVLQTLESRP---SNFHVLYNLDLSIKDKIAKIATEIYGADGVNYTAEADKAIQR
                   **       *           * **  *  **  *   ***** *     * * *

FTHFS_1          LEELGFKNVPVCIAKTQYSLTDDPKLLGRPTGFKINVRNVKISAGAGFVVALTGAIMTMP
FTHFS_2          LEKLGFGKMPVCIAKTQYSLTDDPKKLGRPSGFNITVRDVSVSAGAGFIVAVTGDIMKMP
FTHFS_M.TH.      YESLGYGNLPVVMAKTQYSFSDDMTKLGRPRNFTITVREVRLSAGGRLIVPITGAIMTMP
                  * **    **  ******  **   ****  * * ** *  ***    *  ** ** **

FTHFS_1          GLPKRPAAEKIDVDVNGKIAGLF
FTHFS_2          GLPKVPAAEKIDVDEKGVISGLF
FTHFS_M.TH.      GLPKRPAACNIDIDADGVITGLF
                 **** ***  ** *  * * ***
```

Figure 20. Amino acid sequence alignment of FTHFS 1, FTHFS 2 and the FTHFS from *M.thermoacetica* (M.TH). Conserved residues among compared protein sequences have a star under "*" and those identical in ATP binding proteins are shown in red.

Discussions

FTHFS 1 and FTHFS 2 solubility

The *T. acetatoxydans'* FTHFS 1 and FTHFS 2 protein sequences contain seven and six free cysteine residues respectively, and after examining the structures it was found that none of them participate in disulfide bond formation. This explains also the successful expression of both enzymes in *E.coli*, which is known to have problems with expressing correctly folded recombinant proteins that have disulfide bridges (Baneyx 1999). The high number of free cysteine residues in the two FTHFS proteins made these proteins extremely easy to precipitate, especially in higher concentrations. Consequently a reductant, such as DTT, had to be used in order to keep the proteins soluble (Cleland 1964).

FTHFS 1 and FTHFS 2 formylation activity experiments

Effectiveness of BME
In the study by Rabinowitz and Pricer, 1962 there was evidence that a very high concentration of BME was needed for the formylation reaction, likely for protection of the enzyme against inactivation by heavy metals (Rabinowitz and Pricer, 1962; Himes and Rabinowitz 1962). We have also performed such experiments in a previous study (data not shown) where we could see that the formylation reaction was not proceeding without an extra addition of BME. In this study we have solved the proteins solubility problem for FTHS 1 and 2 by adding DTT to the samples of these, and tried to run the formylation reaction without additional BME (Figure 8). The results clearly showed that additional BME is not needed and that the role of BME probably only was to create a reduced environment needed for keeping the proteins soluble in solution.

Temperature – and pH optimum
The temperature optimum for both FTHFS 1 and FTHFS 2 was estimated to be 60ºC. FTHFS 1 had a pH optimum of 9.0 and FTHFS 2 had a pH optimum of 7.5. An

interesting observation was that a major drop in catalytic activity for FTHFS 1 occurred at pH 7 (figure 9). That experiment was performed several times using different buffers and all showed the same drop in activity at this pH. Since, this bacterium has two FTHFS enzymes and both of them operate in the same pathway there is a possibility that at certain pH levels the activity of these enzymes shifts depending on the environmental conditions. Soaking crystals of FTHFS 1 with substrates, solve their structures and investigate the interactions between enzyme and substrates may give an explanation of the activity drop at pH 7.5 for FTHFS 1. Molecular docking programs may also be used for investigating potential changes for example in bindings strength during the pH shift. Other possible reasons to this phenomenon may be found by looking at the pKa values of the amino acids involved in building up the catalytic center of the enzymes, and for the substrates. Last but not least, it may be the oligomeric state of the enzyme that is shifting at different pH's , for example from an active dimer to a less active tetramer. To answer this question, we have to find out the oligomeric state of an active FTHFS 1 and FTHFS 2 in solution. That can be done for example by a dynamic light scattering method (DLS) (Berne and Pecora 2000).

PH optimum together with different buffers
Activity measurements performed using different buffers at variable pH (table 1 and 2) showed that FTHFS 2 had the highest activity in a HEPES buffer, pH 7.5, and for FTHFS 1 in a tricine buffer, pH of 9.0. Surprisingly, bicine and bis-tris propane buffers at pH 9.0 showed a strong decrease in activity of FTHFS 1 compared to the tricine buffer at pH 8.3. Interestingly, tricine buffer that was more favorable for FTHFS 1 was less favorable for FTHFS 2. Thus, it seemed that the buffers themselves had an inhibitory effect on both FTFHS 1 and FTHFS 2 activity.

Enzymes activity measurements were done to see how saturated the enzymes are at different concentrations. The reason why the absolute absorbance levels on the graphs in figure 9 and 11 were lower during pH and temperature optimum determination, compared to the ones for FTHFS 2, was that we had used 1000 times less concentrated FTHFS 1 in these experiments compared to the same experiment carried out with FTHFS 2.

FTHFS 1 and FTHFS 2 deformylation activity experiments

Deformylation reactions
Deformylation reactions with FTHFS 1 and FTHFS 2 were performed, as described in (Shoaf, et al. 1974), measuring the disappearance of the product – FTHF. Since we had experienced troubles in running the deformylation reaction in a previous study (unpublished results), some adjustments to the experiment in this study were made. Phosphate was replaced by arsenate and a cysteine was added to the reaction mixture. Arsenate was used because of its ability to stop the accumulation of ATP (Delnomdedieu et al. 1994; Winski and Carter 1998), which might be produced in small quantities since we are trying to run the reaction in the reverse direction (figure 4). Arsenate shares also similar biochemical properties with phosphate (Henry B.F 1996). There was a drop in activity occurring after 10 seconds of measurement using FTHFS 2 enzyme (figure 15) compare to the experiments using FTHFS 1 (figure 16) pointing towards that a deformylation reaction occurs, but this is not a solid proof for that the reaction has occurred. However, this experiment was only carried out once, so

this experiment needs to be repeated in triplicates to get decent standard deviation values. Furthermore, it was also difficult to perform this experiment du to experimental setup problems, and specifically manage to take one or several measurement between time point 0 and 10, seconds using our experimental techniques. The reduction of the enzyme concentration did not slow down the reaction speed either (data no shown).

To find out what actually happens during these first 10 seconds of reaction a new method of measurements has to be tried. Using "stopped-flow" equipment system we will be able to measure milliseconds of the reaction. Since, ATP is one of the products of the deformylation reaction another approach of confirming at least the first step in the reaction may be introduced. Instead of measuring the disappearance of FTHF during the reaction there is a possibility to measure the formation of ATP by using an ATP measuring kit to confirm the deformylation process. Maybe there is even a possibility to couple the formation of ATP to some other reaction that will consume newly synthesized ATP for their own purpose, and with that, process our deformylation reaction.

FTHFS 1 and FTHFS 2 structures solution and refinement

A homology model was made of FTHFS 2 using the I-TESSER (Zhang 2009) program server and the structure of FTHFS 2 was solved using this homology model by molecular replacement, to 2.9 Å resolution, using an x-ray dataset collected on beamline I911-X at MAX-Lab. The auto-build function in the program package PHENIX was not able to build FTHFS 2 properly because the dataset had to low resolution, so we had to either build the structure manually or collect higher resolution data. Since time was limited and manual building would be tedious we aimed for getting better crystals that would diffract to a higher resolution. Meanwhile trying to get better diffracting crystals of FTHFS 2, we got crystals of FTHFS 1 that diffracted to 2.15 Å resolution. So we shifted priority and worked on the structure of FTHFS 1 instead. Since the sequence identities between FTHFS 1 and FTHFS 2 were 73% a polyalanin model of the recently solved FTHFS 2 was used to solve the FTHFS 1 structure by molecular replacement using the program Phaser in the CCP4 program suite. PHENIX was then able to automatically build a nearly complete structure model of FTHFS 1, which after preliminary refining had an R and R_{free} of 21.5% and 25.2%, respectively. New and better crystals of FTHFS 2 were then obtained that diffracted to 2.3Å resolution. A polyalanin model of the recently solved FTHFS 1 structure was then used as input model for Phenix autobuild. The program built a nearly complete model of the FTHFS 2 structure that has been partially refined to 2.3Å resolution with a current R and R_{free} value of 23.3% and 28.8%, respectively.

Both structures need further refinement such as adjustments of amino acid residues, addition of double conformations, finding waters, PEG and metal molecules. Refinement of all these components will make the R and Rfree values drop even more resulting in a more accurate structure formation.

Next step in structure characterization of FTHFS 1 and 2 would be to try to co-crystallize these enzymes with different substrate ligands bound to the enzymes and analyze these ligand bound structures.

Prediction studies of active sites of FTHFS 1 and FTHFS 2

The amino acid sequence alignment of several different FTHFS sequences from different organisms (Lovell et al. 1990) together with the FTHFS sequences from *M. thermoacetica* and with some ATP binding proteins proposed the ATP binding site (Radfar et al. 2000). Considering the previous sequence alignment analysis of ATP binding amino acids from *M. thermoacetica* a similar alignment was performed including FTHFS 1 and FTHFS 2 indicating putative ATP binding amino acids (figure 20).

FTHFS from *M. thermoacetica* had been co-crystallized with substrates bound in the proposed active site of the enzyme (Celeste et al. 2012), revealing, among other things, a putative binding sites for formylphosphate (XPO) and ADP, which was the first step of the formylation reaction mechanism. Superposition of the product complex XPO-ADP from *M. thermoacetica* to the structures of FTHFS 1 and FTHFS 2, showed in figure 21, had rmsd values of 1.54 Å and 1.56 Å, respectively. Since the structural composition of different FTHFS proteins were so similar the putative active site of FTHFS 1 and FTHFS 2 could easily be predicted, as shown in figure 22. Moreover, we also believe that the same amino acids that bind the formylphosfate and ADP ligand in *M. thermoacetica* are involved in binding of the formylphosfate and ADP ligand in FTHFS 1 and FTHFS 2, since these amino acids are mainly conserved. The formylphosfate and ADP, from the *M. thermoacetica* ligand bound structure (PDB code 3RBO), fits nicely in the active binding channel site of FTHFS 1 and FTHFS 2 (figure 23). However, soaking of FTHFS 1 and FTHFS 2 with the substrates and structure solution is necessary to draw further more reliable conclusions about ligand binding in FTHFS 1 and FTHFS 2, since these two structures may probably change their conformation upon binding of substrates.

Figure 21. Panel A: Monomeric structure of the FTHFS from *M. thermoacetica* (green, PDB code 3PZX) together with the ligands of formylphosphate (XPO) and ADP (black) that are superposed on FTHFS 1 NCS molecule A (yellow), with a rmsd value of 1.54 Å, and FTHFS 2 NCS molecule A (pink), with an rmsd value of 1.56 Å. The super positioning of the bound ligands in *M. thermoacetica* structure is indicating a possible active site pocket of FTHFS 1 and FTHFS 2. Panel B: Superposition of FTHFS 1 on FTHFS 2 with an rmsd value of 0.70 Å.

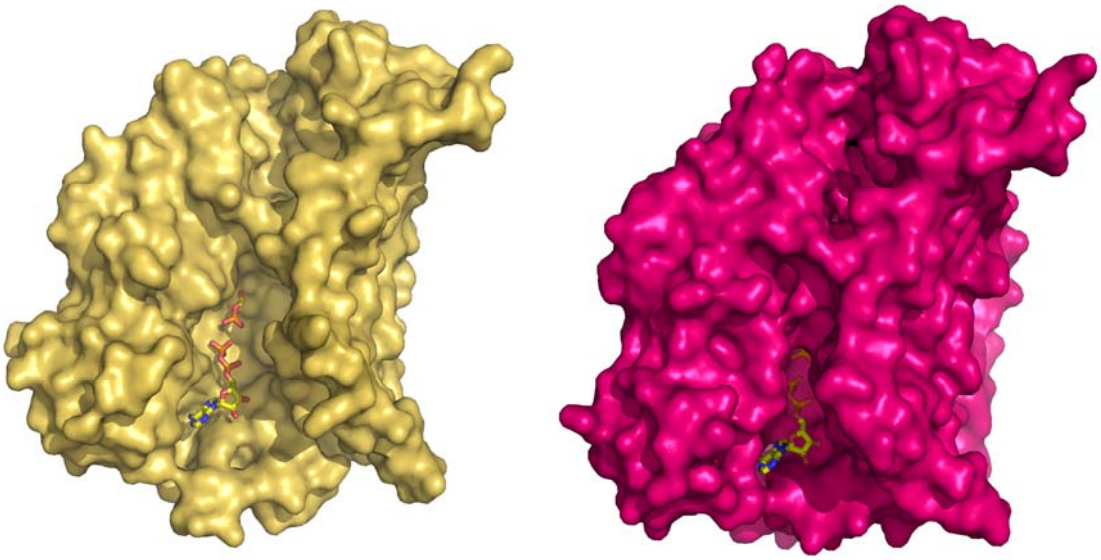

Figure 22. Surface representation of FTHFS 1 (yellow) and FTHFS 2 (pink). Formylphosphate and ADP, shown as sticks, from the ligand bound structure of *M. thermoacetica* (PDB code 3RBO) are superpositioned on the putative active site of FTHFS 1 and FTHFS 2.

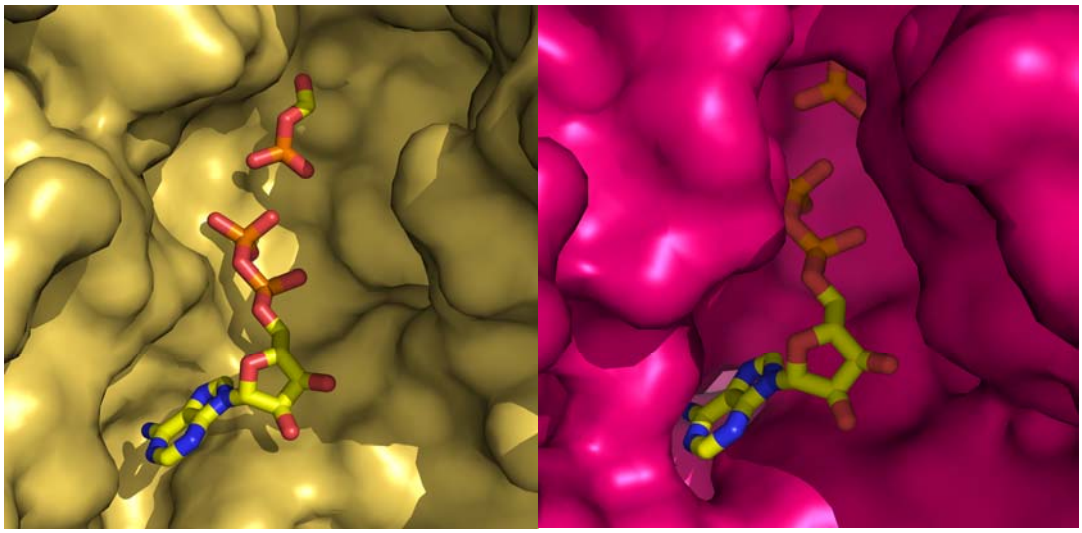

Figure 23. A close up of surface representation of FTHFS 1 (yellow) and FTHFS 2 (pink). Formylphosphate and ADP, shown as sticks, from the ligand bound structure of *M. thermoacetica* (PDB code 3PZX), are super positioned on the putative active site of FTHFS 1 and FTHFS 2.

Conclusions

The mesophilic bacterium, *Tepidanaerobacter acetatoxydans Re1*, unexpectedly shows a temperature optimum of 60°C for some of its key enzymes, FTHFS 1 and FTHFS 2. This means that the yield of FTHF, the formylation product, is obtained most effectively at 60°C. The pH optimum in the formylation reaction for FTHFS 1 is determined to pH 7.5, using HEPES as a buffer system, while FTHFS 2 has a pH optimum of 9.0, using tricine buffer system.

Looking at figure 15 we can see that the activity of FTHFS 2 is to fast, while the deformylation reaction catalyzed by FTHFS 1 can not be shown. New strategies of

measuring the deformylation reaction have to be tried, such as “stop-flow” measurement method.

The FTHFS 1 structure was solved to a resolution of 2.15 Å, and FTHFS 2 was solved to 2.30 Å resolution. FTHFS 1 contains four NCS protein molecules in the asymmetric unit, while FTHFS 2 has two. Tetrameric FTHFS 1 is arranged by two 2-fold and one 4-fold noncrystallographic symmetry in the asymmetric unit. Dimeric FTHFS 2 is arranged by one 2-fold noncrystallographic symmetry in the asymmetric unit. There is no electron density for some of the amino acids in both enzymes, so more refinement has to be done.

Acknowledgment

This research was supported by the thematic research program MicroDrive at SLU, Uppsala.

I would like to thank Jerry Ståhlberg, Saeid Karkehabadi, Henrik Hansson for their very supportive discussions and helpful advices and my supervisor Nils Egil Mikkelsen for teaching me crystallization and structure determination techniques. I would also like to thank Anna Schnürer, Bettina Müller for the opportunity to work on their project and Mats Sandgren for inviting me into his group to perform all of the experiments.

References

Adams, P. D., P. V. Afonine, et al. (2010). "PHENIX: a comprehensive Python-based system for macromolecular structure solution." Acta Crystallogr D Biol Crystallogr **66**(Pt 2): 213-221.

Balk, M., J. Weijma, et al. (2002). "Thermotoga lettingae sp. nov., a novel thermophilic, methanol-degrading bacterium isolated from a thermophilic anaerobic reactor." Int J Syst Evol Microbiol **52**(Pt 4): 1361-1368.

Baneyx, F. (1999). "Recombinant protein expression in Escherichia coli." Curr Opin Biotechnol **10**(5): 411-421.

Bergfors, T. (2003). "Seeds to crystals." J Struct Biol **142**(1): 66-76.

Bergfors, T. M. (1999). Precipitants. Protein Crystallization. T. M. Bergfors**:** 41-46.

Berne, B.J.; Pecora, R. (2000) Dynamic Light Scattering. Courier Dover Publications

Celeste, L. R., G. Chai, et al. (2012). "Mechanism of N(10) -formyltetrahydrofolate synthetase derived from complexes with intermediates and inhibitors." Protein Sci **21**(2): 219-228.

Cleland, W. W. (1964). "Dithiothreitol, a New Protective Reagent for Sh Groups." Biochemistry **3**: 480-482.

(CCP4 1994). "The CCP4 suite: programs for protein crystallography." Acta Crystallogr D Biol Crystallogr **50**(Pt 5): 760-763.

DeLano, W. L. (2002). The PyMOL molecular graphics system. S. LLC. New York.

Delnomdedieu, M., M. M. Basti, et al. (1994). "Complexation of arsenic species in rabbit erythrocytes." Chem Res Toxicol **7**(5): 621-627.

Drenth, J. (1994). Principles of Protein X-ray Crystallography.

Emsley, P. and K. Cowtan (2004). "Coot: model-building tools for molecular graphics." Acta Crystallogr D Biol Crystallogr **60**(Pt 12 Pt 1): 2126-2132.
Evans, P. (2006). "Scaling and assessment of data quality." Acta Crystallogr D Biol Crystallogr **62**(Pt 1): 72-82.
Ferry, J. G. (1992). "Biochemistry of methanogenesis." Crit Rev Biochem Mol Biol **27**(6): 473-503.
Garman, E. F. (1999). Crystallization for Cryo-Data Collection. Protein Crystallization. T. Bergfors**:** 183-185.
Gale R (1993). *Crystallography Made Crystal Clear*. Academic Press.
Hattori, S. (2008). "Syntrophic acetate-oxidizing microbes in methanogenic environments." Microbes Environ **23**(2): 118-127.
Hattori, S., Y. Kamagata, et al. (2000). "Thermacetogenium phaeum gen. nov., sp. nov., a strictly anaerobic, thermophilic, syntrophic acetate-oxidizing bacterium." Int J Syst Evol Microbiol **50 Pt 4**: 1601-1609.
Henry B.F, D. (1996). The Biochemical Action of Arsonic Acids Especially As Phosphate Analogues. Advances in Inorganic Chemistry. A. G. Sykes, Academic Press. **Volume 44:** 191-227.
Himes, R. H. and J. A. Harmony (1973). "Formyltetrahydrofolate synthetase." CRC Crit Rev Biochem **1**(4): 501-535.
Himes, R. H. and T. Wilder (1965). "Formyltetrahydrofolate synthetase: mechanism of cation activation." Biochim Biophys Acta **99**(3): 464-475.
Hum, D. W., A. W. Bell, et al. (1988). "Primary structure of a human trifunctional enzyme. Isolation of a cDNA encoding methylenetetrahydrofolate dehydrogenase-methenyltetrahydrofolate cyclohydrolase-formyltetrahydrofolate synthetase." J Biol Chem **263**(31): 15946-15950.
Jetten, M. S. M., A. J. M. Stams, et al. (1992). "Methanogenesis from acetate: a comparison pf the acetate metabolism in *Methanothrix soehngenii* and *Methanosacrina* " FEMS Microbiol. Lett. **88 (3-4)**: 181 - 197.
Kabsch, W. (2010). "Xds." Acta Crystallogr D Biol Crystallogr **66**(Pt 2): 125-132.
Lee, M. J. and S. H. Zinder (1988). "Isolation and Characterization of a Thermophilic Bacterium Which Oxidizes Acetate in Syntrophic Association with a Methanogen and Which Grows Acetogenically on H(2)-CO(2)." Appl Environ Microbiol **54**(1): 124-129.
Lewinski, K., Y. Hui, et al. (1993). "Crystallization and preliminary crystallographic data for formyltetrahydrofolate synthetase from Clostridium thermoaceticum." J Mol Biol **229**(4): 1153-1156.
Ljungdahl, L. (1994). The acetyl-CoA pathway and the chemiosmotic generation of ATP during acetogenesis. Acetogenesis. H. Drake. New York, Chapman and Hall**:** 63–87.
Ljungdahl, L. G. (1986). "The autotrophic pathway of acetate synthesis in acetogenic bacteria." Annu Rev Microbiol **40**: 415-450.
Lovell, C. R., A. Przybyla, et al. (1990). "Primary structure of the thermostable formyltetrahydrofolate synthetase from Clostridium thermoaceticum." Biochemistry **29**(24): 5687-5694.
MacKenzie, R. E. (1984). Biogenesis and interconversion of substituted tetrahydro-folate. Folates and pterins: Chemistry and biochemistry of folates. New York, In: Blakely R., Benkovic S. **1:** 255 - 306.
MacKenzie, R. E. and J. C. Rabinowitz (1971). "Cation-dependent reassociation of subunits of N10-formyltetrahydrofolate synthetase from Clostridium acidi-urici and Clostridium cylindrosporum." J Biol Chem **246**(11): 3731-3736.
McCarty, P. L. (1964). Anaerobic Waste Treatment Fundamentals.

McCoy, A. J., R. W. Grosse-Kunstleve, et al. (2007). "Phaser crystallographic software." J Appl Crystallogr **40**(Pt 4): 658-674.
McPherson, A. (1999). A bit of advice on crystallizing proteins. Protein Crystallization. T. M. Bergfors**:** 3-6.
Murshudov, G. N., A. A. Vagin, et al. (1997). "Refinement of macromolecular structures by the maximum-likelihood method." Acta Crystallogr D Biol Crystallogr **53**(Pt 3): 240-255.
Oryx6. (2012). "Douglas Instruments Ltd." from http://www.douglas.co.uk/.
Paukert, J. L., L. D. Straus, et al. (1976). "Formyl-methyl-methylenetetrahydrofolate synthetase-(combined). An ovine protein with multiple catalytic activities." J Biol Chem **251**(16): 5104-5111.
Rabinowitz, J. C. and W. E. Pricer, Jr. (1962). "Formyltetrahydrofolate synthetase. I. Isolation and crystallization of the enzyme." J Biol Chem **237**: 2898-2902.
Radfar, R., A. Leaphart, et al. (2000). "Cation binding and thermostability of FTHFS monovalent cation binding sites and thermostability of N10-formyltetrahydrofolate synthetase from Moorella thermoacetica." Biochemistry **39**(47): 14481-14486.
Radfar, R., R. Shin, et al. (2000). "The crystal structure of N(10)-formyltetrahydrofolate synthetase from Moorella thermoacetica." Biochemistry **39**(14): 3920-3926.
Ragsdale, S. W. (1997). "The eastern and western branches of the Wood/Ljungdahl pathway: how the east and west were won." Biofactors **6**(1): 3-11.
Ragsdale, S. W. and E. Pierce (2008). "Acetogenesis and the Wood-Ljungdahl pathway of CO(2) fixation." Biochim Biophys Acta **1784**(12): 1873-1898.
Roche. (2012). "Roche Applied Science." from https://www.roche-applied-science.com/servlet/StoreFramesetView?langId=-1&storeId=10305&catalogId=10304&krypto=Rr5SjK5PGh5I9DITh2MH8g%3D%3D&ddkey=https:RCConfigureUser.
Schink, B. (1997). "Energetics of syntrophic cooperation in methanogenic degradation." Microbiol Mol Biol Rev **61**(2): 262-280.
Schirch, L. (1978). "Formyl-methenyl-methylenetetrahydrofolate synthetase from rabbit liver (combined). Evidence for a single site in the conversion of 5,10-methylenetetrahydrofolate to 10-formyltetrahydrofolate." Arch Biochem Biophys **189**(2): 283-290.
Schnurer, A. and A. Nordberg (2008). "Ammonia, a selective agent for methane production by syntrophic acetate oxidation at mesophilic temperature." Water Sci Technol **57**(5): 735-740.
Schnurer, A., B. Schink, et al. (1996). "Clostridium ultunense sp. nov., a mesophilic bacterium oxidizing acetate in syntrophic association with a hydrogenotrophic methanogenic bacterium." Int J Syst Bacteriol **46**(4): 1145-1152.
Scott, J. M. and J. C. Rabinowitz (1967). "The association-dissociation of formyltetrahydrofolate synthetase and its relation to monovalent cation activation of catalytic activity." Biochem Biophys Res Commun **29**(3): 418-423.
Shoaf, W. T., S. H. Neece, et al. (1974). "Effects of temperature and ammonium ions on formyltetrahydrofolate synthetase from Clostridium thermoaceticum." Biochimica et Biophysica Acta (BBA) - Enzymology **334**(2): 448-458.
Sievers, F., A. Wilm, et al. (2011). "Fast, scalable generation of high-quality protein multiple sequence alignments using Clustal Omega." Mol Syst Biol **7**: 539.

Sly, W. S. and E. R. Stadtman (1963). "Formate Metabolism. Ii. Enzymatic Synthesis of Formyl Phosphate and Formyl Coenzyme a in Clostridium Cylindrosporum." J Biol Chem **238**: 2639-2647.

Tan, L. U. and R. E. Mackenzie (1977). "Methylenetetrahydrofolate dehydrogenase, methenyltetrahydrofolate cyclohydrolase and formyltetrahydrofolate synthetase from porcine liver. Isolation of a dehydrogenase-cyclohydrolase fragment from the multifunctional enzyme." Biochim Biophys Acta **485**(1): 52-59.

Tanner, R. S. and C. R. Woese (1994). A phylogenetic assessment of the acetogens. Acetogenesis. H. L. Drake. New York, Chapman and Hall**:** 254-272.

U.S. Energy Information Administration (EIA), t. s. a. The International Energy Outlook 2010 (IEO2010). The statistical and analytical agency within the U.S. Department of Energy. Washington, DC 20585.

UK'sBiocentre. "UK's national centre for renewable fuels, materials and technologies." from http://www.nnfcc.co.uk/metadot/index.pl.

Unge, T. (1999). Crystallization methods. Protein Crystallization. T. M. Bergfors**:** 9-15.

Welch, W. H., C. L. Irwin, et al. (1968). "Observations on the monovalent cation requirements of formyltetrahydrofolate synthetase." Biochem Biophys Res Commun **30**(3): 255-261.

Westerholm, M., Müller, B. et al. (2011). Syntrophic acetate-oxidizing bacteria in biogas digesters - quantification and detection. International Conference on Biogas Microbiology. Germany.

Westerholm, M., S. Roos, et al. (2010). "Syntrophaceticus schinkii gen. nov., sp. nov., an anaerobic, syntrophic acetate-oxidizing bacterium isolated from a mesophilic anaerobic filter." FEMS Microbiol Lett **309**(1): 100-104.

Westerholm, M., S. Roos, et al. (2010). *Tepidanaerobacter acetatoxydans* sp. nov., an anaerobic, syntrophic acetate - oxidizing bacterium isolated from two ammonium - enriched mesophilic methanogenic processes. Uppsala, Swedish University of Agricultural Sciences.

White, D. (1995). The Physiology and Biochemistry of Prokaryotes. New York, Oxford University Press.

Winski, S. L. and D. E. Carter (1998). "Arsenate toxicity in human erythrocytes: characterization of morphologic changes and determination of the mechanism of damage." J Toxicol Environ Health A **53**(5): 345-355.

Zhang, Y. (2009). "I-TASSER: fully automated protein structure prediction in CASP8." Proteins **77 Suppl 9**: 100-113.

Zinder, S. and M. Koch (1984). "Non - aceticlastic methanogenesis from acetate: acetate oxidation by a syntrophic acetate oxidation by a thermophilic syntrophic coculture." Arch Microbiol **138**: 263 - 272.

Formyl – tetrahydrofolatesynthetase (FTHFS) – ett nyckelprotein i biokemiska reaktioner under biogasprocessen.

Biogas, som består av metan och koldioxid är en förnybar energikälla som kan användas bland annat för produktion av drivmedel eller elektricitet. Biogas bildas genom mikrobiell nedbrytning av olika typer av organiska material, exempelvis olika grödor och hushållavfall, i frånvaro av syre. Strävan efter att ersätta fossila bränslen med förnyelsebara har lett till att biogasproduktionen stadigt ökar i hela Europa. Ett vanligt problem under biogasframställningen är processinstabilitet orsakad av höga halter av ammoniak, som kommer från proteinrika produkter såsom slakteriavfall, och vissa gödselfraktioner som används vid biogasproduktion. Ammoniak är giftigt för flera olika organismer som är inblandade i biogasproduktionen. Vissa organismer klarar dock av att leva vid höga halter av ammoniak, en av dessa är *Tepidanaerobacter acetatoxydans Re1*. Tillsammans med andra mikroorganismer, metanogener, producerar de biogas i biogasanläggningar även vid relativt höga ammoniakhalter. För att vara mer detaljerad kan man säga att *Tepidanaerobacter acetatoxydans Re1* framställer koldioxid och vätgas. Metanogener använder sig utav vätgasen och omvandlar koldioxid till metan.

Ett protein, som heter formyl – tetrahydrofolatesynthetase (FTHFS), spelar en viktig roll för funktionen hos vissa bakterier, och inte minst hos *Tepidanaerobacter acetatoxydans Re1*. Det som i dagsläget kännetecknar denna unika bakteriestamm är att den har två olika proteinvarianter av FTHFS, vilket helt nyligen har blivit upptäckt. Vi tror att anledningen till att denna organism har två FTHFS enzymer är de tuffa förhållanden som råder under biogas framställning från proteinrika material. Den höga ammoniumhalten gynnar tillväxten och koldioxid produktionen främst hos de bakteriestammar som har två varianter av FTHFS enzymer. Denna observation tillåter oss att ha hypotesen att ett av FTHFS proteinerna är funktionellt och andra är hämmade under de olika förhållandena.

Denna studie gick framförallt ut på att genomföra olika biokemiska karaktäriseringar, kristallisera och lösa de tredimensionella strukturerna utav FTHFS 1 och FTHFS 2 från *Tepidanaerobacter acetatoxydans Re1*. De biokemiska karaktäriseringarna, dvs. att se hur proteinernas aktivitet påverkas under olika omständigheter som liknar de som råder i en biogasanläggning, genomfördes för att försöka karaktärisera dem båda enzymerna. Vid dessa experiment testade vi vilket temperatur och pH som är bäst för att FTHFS 1 respektive FTHFS 2 ska fungera mest optimalt. Sedan löste vi den tredimensionella strukturen av FTHFS 1 och FTHFS 2, med hjälp av röntgenkristallografi, för att därigenom kunna se hur deras aminosyrastrukturer se ut tri-dimensionellt. Den tredimensionella strukturen av FTHFS 1 och FTHFS 2 kan användas för att förklara den katalytiska mekanismen hos dessa proteiner och vad som skiljer de två enzymerna från varandra Framtida studier kommer förhoppningsvis att kunna visa hur effektiviteten av FTHFS kan optimeras, och därigenom kunna göra så att biogasproduktionen från proteinrika material förbättras.